Architectures for Integrable Quantum Systems

Angela Foerster

Universidade Federal do Rio Grande do Sul
Instituto de Física, Porto Alegre

talk presented at "Challenges in Integrability"
Wuhan, November, 2025

OUTLINE

1- Introduction

2- Integrable bosonic quantum tunneling models

3- Application in a static frame: 4-sites in a ring: NOON states

4- Application in a rotating frame: 4-sites in a tetrahedral geometry: Quantum Turntable

5- Conclusions

1 - INTRODUCTION

Why are quantum integrable models important?

- *They are the gems of theoretical physics: elegant, insipiring, and relatively scarce.*
- *They offer deep insights for a precise and simplified understanding of many physical properties.*
- *They serve as benchmarks, validating techniques for complex quantum systems.*
- *They can be found in many areas, such as Statistical Physics, QFT, Condensed Matter, Cold Atoms - our focus*

- Here:

  We introduce a family of integrable multi-well quantum tunneling models in cold atoms, and discuss some possible applications.

Why are we studying integrable tunneling models?

They display high potential for applications in the development of emerging quantum technologies:

- Solvability and Control: *Integrable models offer analytical formulae and predictions, enabling precise control of quantum states for robust technology development.*
- Understanding Quantum Correlations: *Integrable models offer a platform for studying and manipulating quantum correlations in quantum computing and communication.*
- Developing Quantum Devices: *Integrable models guide the design and understanding of quantum devices, crucial for the implementation of quantum technologies.*

2 - Integrable quantum tunneling models:

Two wells: Two-site Bose Hubbard Hamiltonian:

$$H = \frac{K}{8}(N_1 - N_2)^2 - \frac{\Delta\mu}{2}(N_1 - N_2) - \frac{\mathcal{E}_J}{2}(a_1^\dagger a_2 + a_2^\dagger a_1)$$

- $N_i = a_i^\dagger a_i$: number of atoms in well $(i = 1, 2)$
- K: atom-atom interaction term
- $\Delta\mu$: external potential
- $\mathcal{E}_J$: tunneling strength

G. Milburn et al, Phys. Rev. A **55** *(1997) 4318; A. Leggett, Rev. Mod. Phys.* **73** *(2001) 307*

A. Tonel, J. Links, A. Foerster, JPA 38 (2005) 1235

The quantum dynamics of the model exhibits tunneling & self-trapping - experiment of Oberthaler et al - 2005

Two-wells: Integrability and BA-solution:

- *This model is integrable; it can be formulated by the Yang-Baxter equation and exactly solved via Bethe ansatz methods.*

Multiple-wells:

- We aim to extend this result to multiple wells.
- Natural candidate: $\mathcal{L}$-site Bose-Hubbard model.
  It is not integrable in general.
- Until recently, there was a belief that constructing integrable multi-well systems was not possible.
- We solved this and found that integrability requires the presence of long-range interactions.
- The algebraic construction of these models is tricky, presenting challenges in obtaining all conserved quantities.

Integrable Multi-well tunneling models:

- 3 wells: Triple well Hamiltonian
- 4 wells: Four-well ring model
- ....
- Multi-well tunneling models

Triple well Hamiltonian:

$$\begin{aligned} H &= U(N_1+N_3-N_2)^2+\Delta\mu(N_1+N_3-N_2) \\ &+ t_1(a_1^\dagger a_2+a_1a_2^\dagger)+t_3(a_2^\dagger a_3+a_2a_3^\dagger) \end{aligned} \tag{1}$$

- $N_i=a_i^\dagger a_i$: number of bosons in well i, $(i=1,2,3)$,

  $N=N_1+N_2+N_3$ is constant, H is invariant by changing the indices 1 and 3
- U: controls on-site and inter-well interac. bet. bosons
- $\Delta\mu$: external potential, $t_i, i=1,3$: tunneling strength:

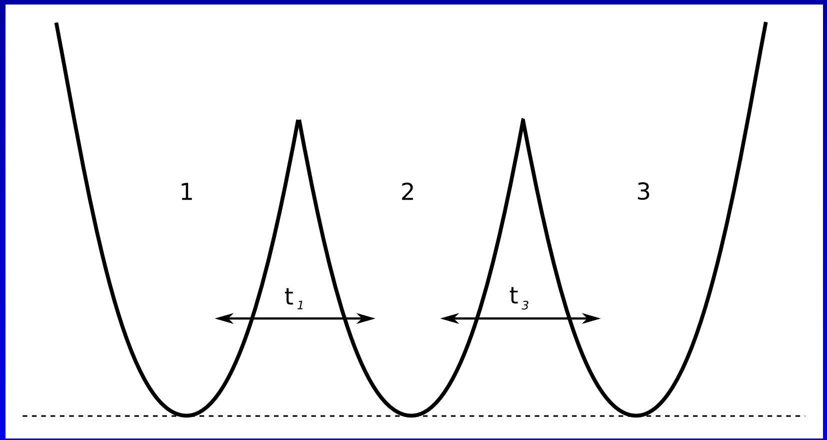

Application: atomtronic switching device

SciPost   SciPost Phys. Core 2, 003 (2020)

Entangled states of dipolar bosons generated in a triple-well potential

Arlei P. Tonel[1], Leandro H. Ymai[1], Karin Wittmann W.[2], Angela Foerster[2] and Jon Links[3⋆]

1 Universidade Federal do Pampa, Bagé, Brazil
2 Instituto de Física da Universidade Federal do Rio Grande do Sul, Porto Alegre, Brazil
3 School of Mathematics and Physics, The University of Queensland, Brisbane, Australia.

⋆ jrl@maths.uq.edu.au

Abstract

We study the generation of entangled states using a device constructed from dipolar bosons confined to a triple-well potential. Dipolar bosons possess controllable, long-range interactions. This property permits specific choices to be made for the coupling parameters, such that the system is integrable. Integrability assists in the analysis of the system via an effective Hamiltonian constructed through a conserved operator. Through computations of fidelity we establish that this approach, to study the time-evolution of the entanglement for a class of non-entangled initial states, yields accurate approximations given by analytic formulae.

COMMUNICATIONS PHYSICS

ARTICLE

DOI: 10.1038/s42005-018-0089-1   OPEN

Control of tunneling in an atomtronic switching device

Karin Wittmann Wilsmann[1], Leandro H. Ymai[2], Arlei Prestes Tonel[2], Jon Links[3] & Angela Foerster[1]

The precise control of quantum systems will play a major role in the realization of atomtronic devices. As in the case of electronic systems, a desirable property is the ability to implement switching. Here we show how to implement switching in a model of dipolar bosons confined to three coupled wells. The model describes interactions between bosons, tunneling of bosons between adjacent wells, and the effect of an external field. We conduct a study of the quantum dynamics of the system to probe the conditions under which switching behavior can occur. The analysis considers both integrable and non-integrable regimes within the model. Through variation of the external field, we demonstrate how the system can be controlled between various "switched-on" and "switched-off" configurations.

Contribution to the blogs of Nature Research Communities:

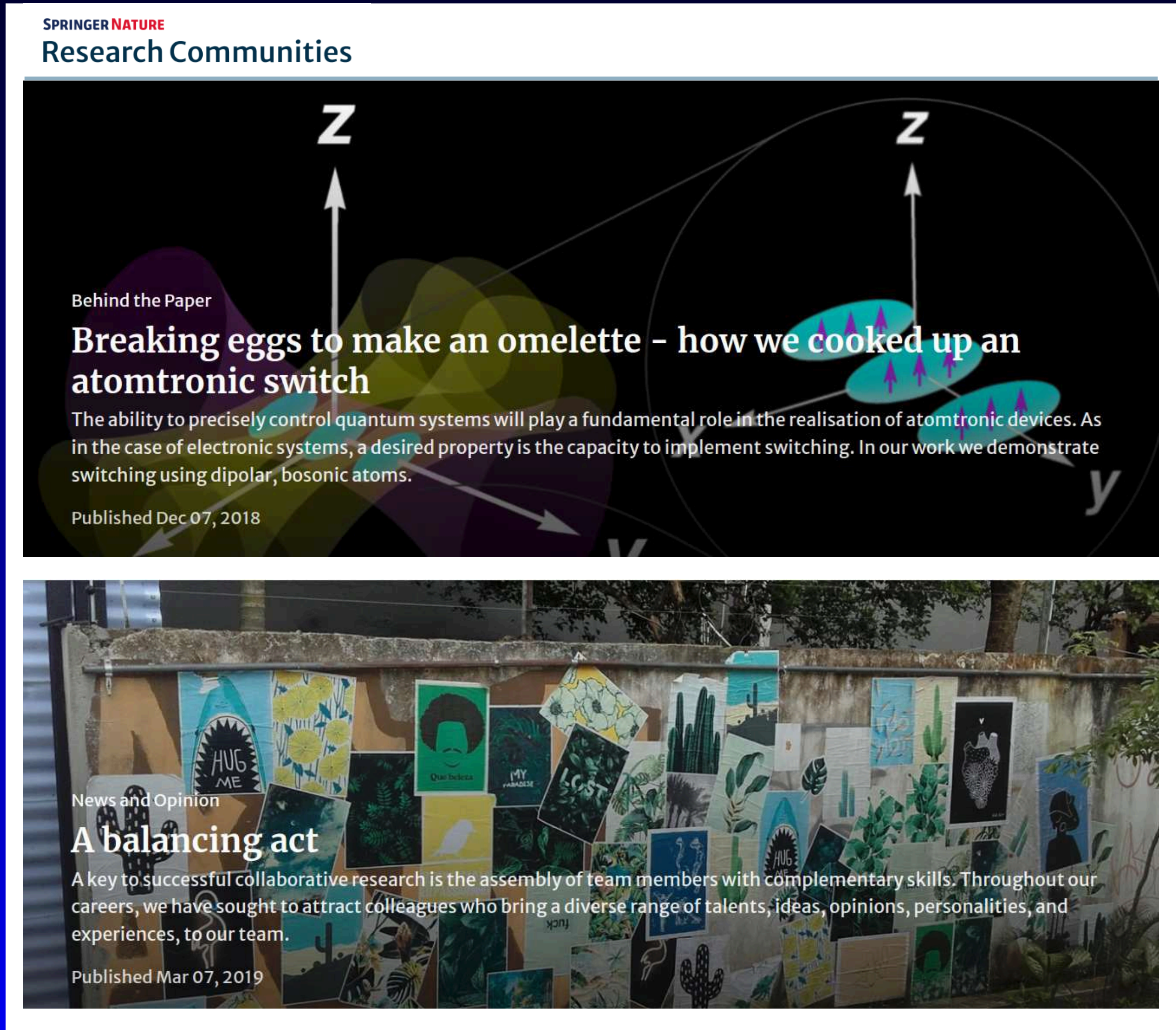

Four-well ring:

$$\begin{aligned} H &= U(N_1+N_3-N_2-N_4)^2 + \Delta\mu(N_1+N_3-N_2-N_4) \\ &+ t_{12}(a_1a_2^\dagger + a_1^\dagger a_2) + t_{14}(a_1a_4^\dagger + a_1^\dagger a_4) \\ &+ t_{23}(a_3a_2^\dagger + a_3^\dagger a_2) + t_{34}(a_3a_4^\dagger + a_3^\dagger a_4) \end{aligned} \tag{2}$$

U: controls on-site and inter-well interactions; t_{ij} are not independent: $t_{12}t_{34} = t_{23}t_{14}$ but still admits sufficient freedom to investigate a range of anisotropic tunneling regimes

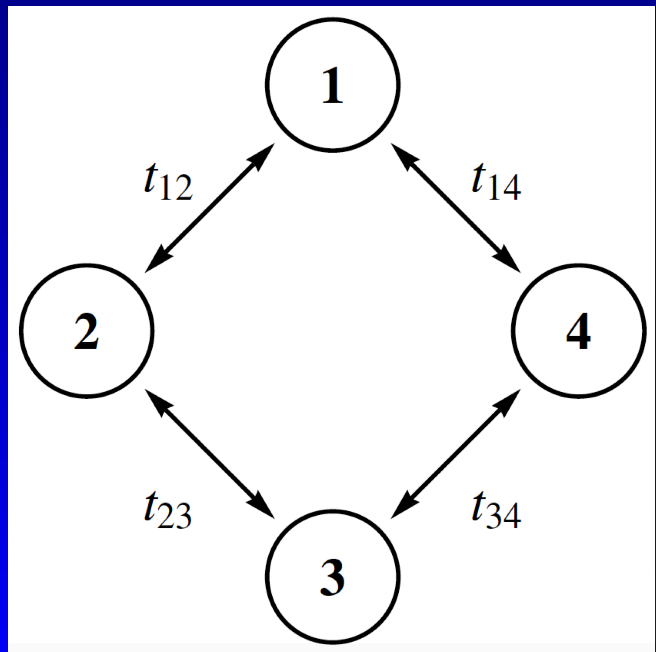

Application: NOON states

PHYSICAL REVIEW LETTERS **129,** 020401 (2022)

Integrable Atomtronic Interferometry

D. S. Grün,[1] L. H. Ymai,[2] K. Wittmann W.,[1] A. P. Tonel,[2] A. Foerster,[1] and J. Links[3,*]
[1]*Instituto de Física da UFRGS, Avenida Bento Gonçalves, 9500 Porto Alegre, Rio Grande do Sul, Brazil*
[2]*Universidade Federal do Pampa, Avenida Maria Anunciação Gomes de Godoy, 1650 Bagé, Rio Grande do Sul, Brazil*
[3]*School of Mathematics and Physics, The University of Queensland, Brisbane 4072, Queensland, Australia*

(Received 9 June 2020; accepted 23 May 2022; published 6 July 2022)

High sensitivity quantum interferometry requires more than just access to entangled states. It is achieved through the deep understanding of quantum correlations in a system. Integrable models offer the framework to develop this understanding. We communicate the design of interferometric protocols for an integrable model that describes the interaction of bosons in a four-site configuration. Analytic formulas for the quantum dynamics of certain observables are computed. These expose the system's functionality as both an interferometric identifier, and producer, of NOON states. Being equivalent to a controlled-phase gate acting on 2 hybrid qudits, this system also highlights an equivalence between Heisenberg-limited interferometry and quantum information. These results are expected to open new avenues for integrability-enhanced atomtronic technologies.

DOI: 10.1103/PhysRevLett.129.020401

communications
physics

ARTICLE
https://doi.org/10.1038/s42005-022-00812-7 OPEN

Protocol designs for NOON states

Daniel S. Grün[1], Karin Wittmann W.[1], Leandro H. Ymai[2], Jon Links[3✉] & Angela Foerster[1]

The ability to reliably prepare non-classical states will play a major role in the realization of quantum technology. NOON states, belonging to the class of Schrödinger cat states, have emerged as a leading candidate for several applications. Here we show how to generate NOON states in a model of dipolar bosons confined to a closed circuit of four sites. This is achieved by designing protocols to transform initial Fock states to NOON states through use of time evolution, application of an external field, and local projective measurements. The evolution time is independent of total particle number, offering an encouraging prospect for scalability. By variation of the external field strength, we demonstrate how the system can be controlled to encode a phase into a NOON state. We also discuss the physical feasibility, via ultracold dipolar atoms in an optical superlattice setup. Our proposal showcases the benefits of quantum integrable systems in the design of protocols.

Contribution to the blog of Nature Research Communities:

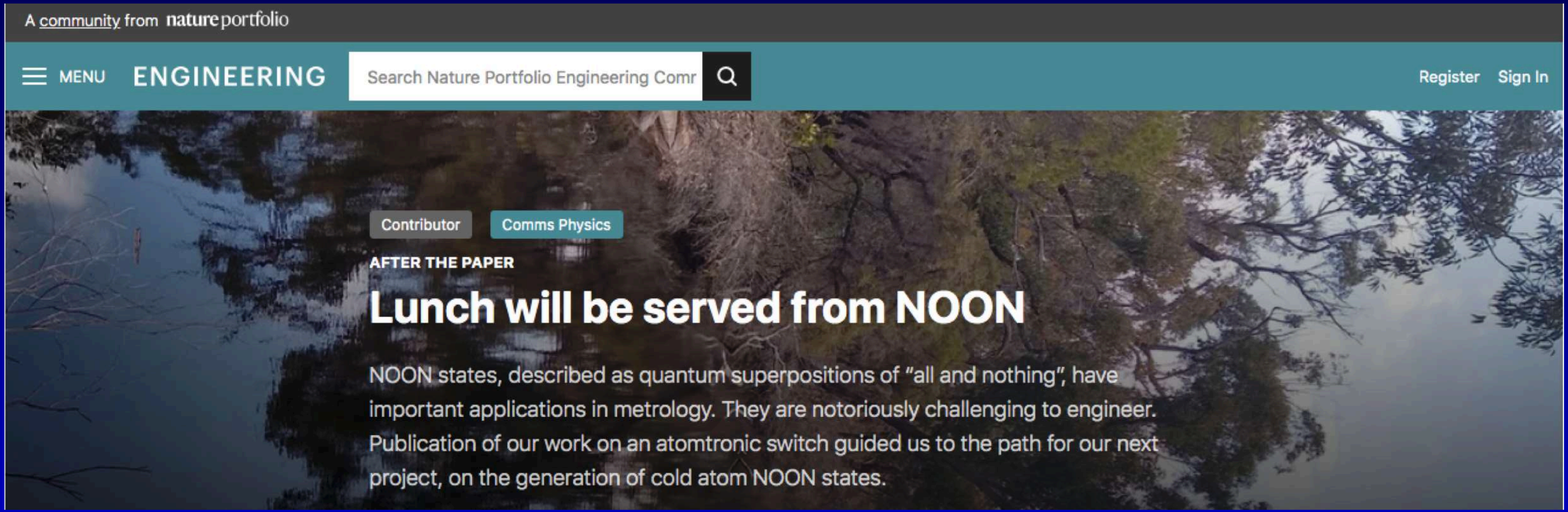

Multi-well tunneling models:

- Hamiltonian for $(n+m)$ wells:

$$H_{n,m} = U(N_A - N_B)^2 + \Delta\mu(N_A - N_B) + \sum_{i=1}^{n}\sum_{j=1}^{m} t_{i,j}(a_i b_j^\dagger + a_i^\dagger b_j)$$

- in terms of sets of canonical boson operators:

$$a_i,\ a_i^\dagger, N_{a,i} = a_i^\dagger a_i,\ i = 1, \ldots, n$$
$$b_j,\ b_j^\dagger,\ N_{b,j} = b_j^\dagger b_j,\ j = 1, \ldots, m$$
$$N_A = \textstyle\sum_{i=1}^{n} a_i^\dagger a_i \quad N_B = \sum_{j=1}^{m} b_j^\dagger b_j \quad N = N_A + N_B$$

- U intra-well and inter-well interaction between bosons
- $\Delta\mu$ external potential, $t_{i,j}$ couplings for tunneling
- Models defined on complete bipartite graphs $K_{n,m}$

Some particular Hamiltonians:

For particular choices of n, m we find

- 2 wells:

  $n = m = 1$: Two-site Bose Hubbard model

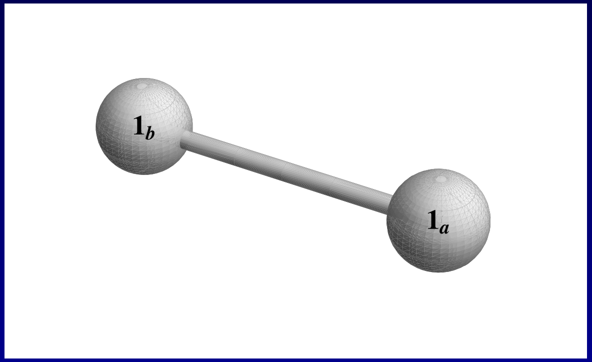

- 3 wells:

  $n = 2, m = 1$: Triple well Hamiltonian

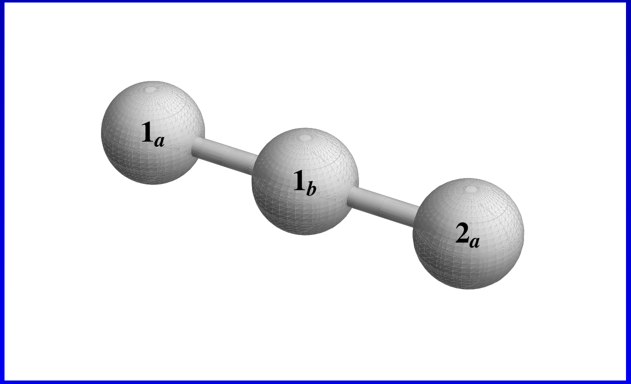

- 4 wells:

  $n = 2, m = 2$: Four-well ring model:

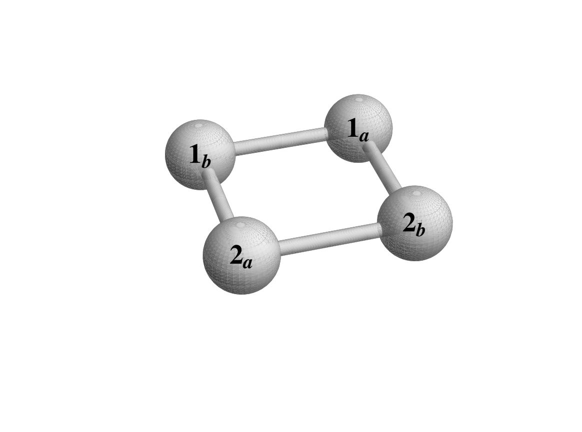

  $n = 3, m = 1$: Open four well model:

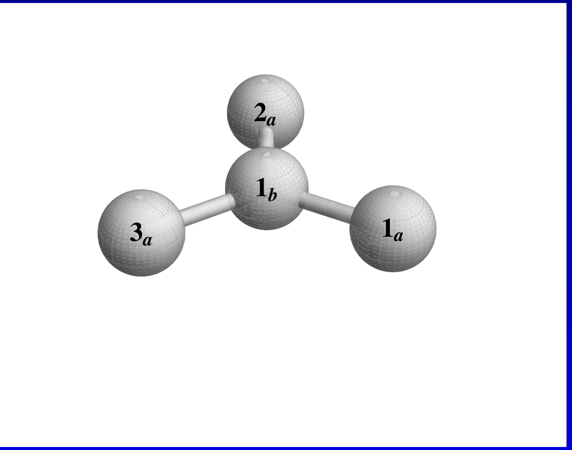

Schematic rep.: spheres represent the wells, with bonds indicating the tunneling between the wells

6 wells: $n = 4, m = 2$:

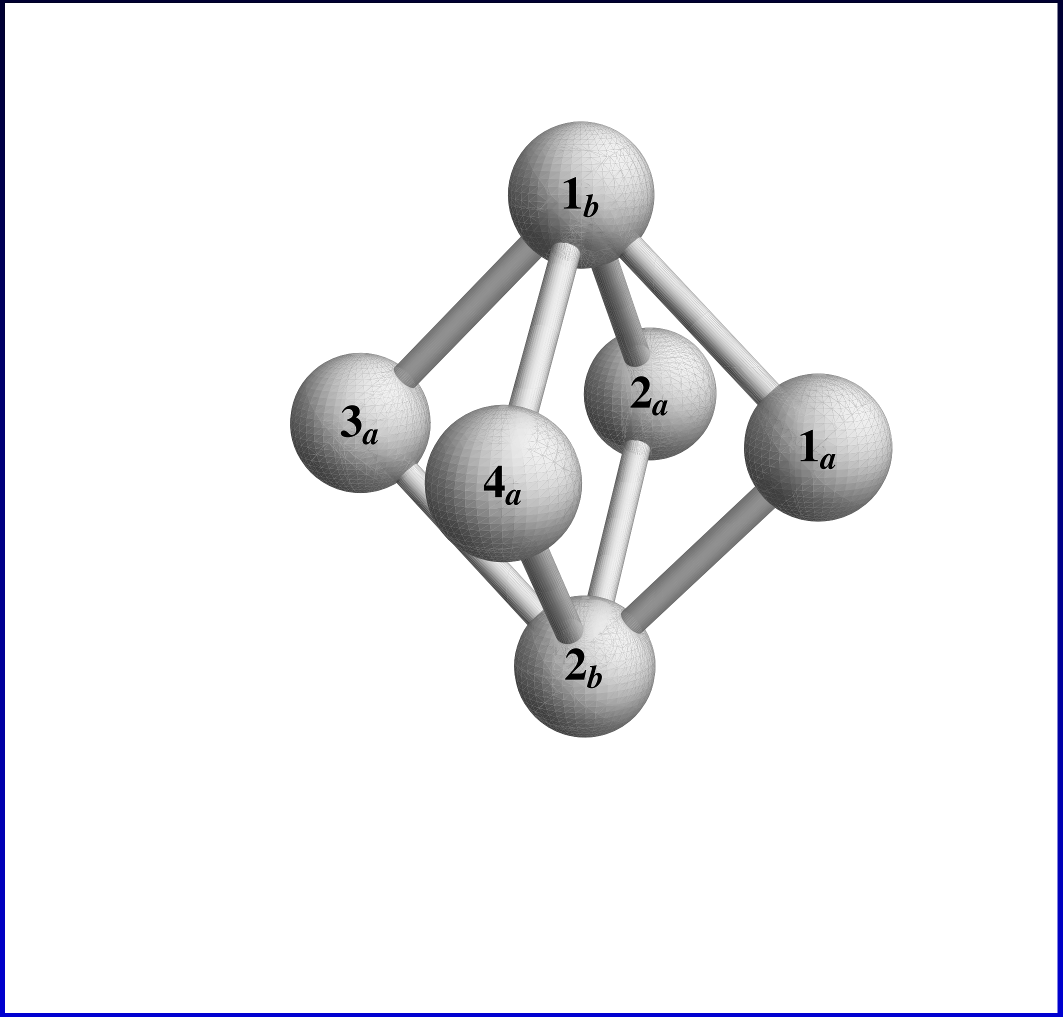

L. Ymai, A. Tonel, A. Foerster, J. Links, JPA 2017

6 wells: $n = 5, m = 1$:

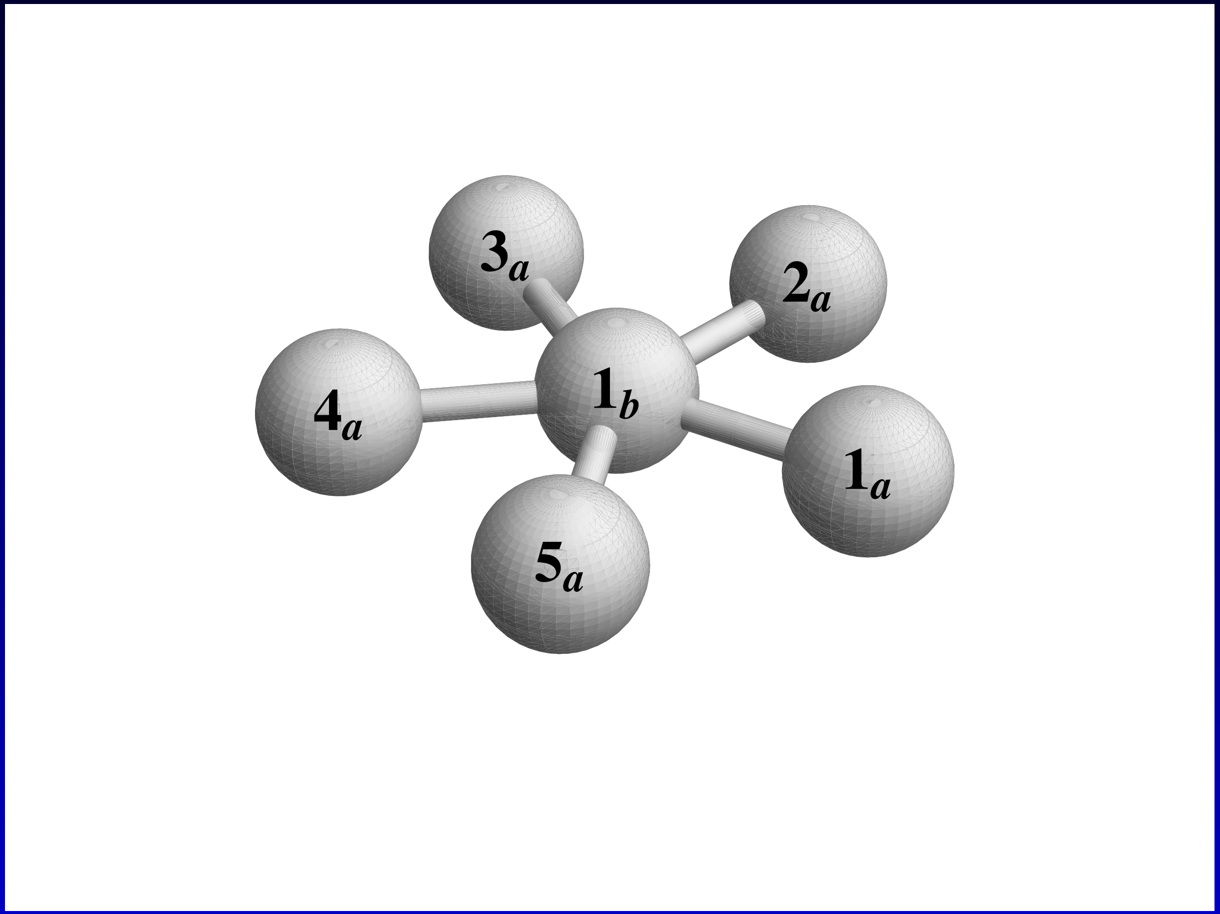

OBS I: EBHM

- These integrable multi-well tunneling models are not toy models. They are particular cases of the Extended-Bose Hubbard Model (EBHM) with $\mathcal{L}$-sites.

OBS II: Superintegrability:

- For $n > 2$ or $m > 2$ the $(n + m)$-wells (or sites) tunneling Hamiltonian is superintegrable:
  more conserved quantities than degrees of freedom.
- The existence of superintegrability allows for the inclusion of additional interaction terms that can break the global symmetry algebra without compromising integrability.
- We can extend the models to include tunneling terms while retaining integrability

Example: $n = 3, m = 1$

- Superintegrable 4-sites in a tetrahedral geometry:

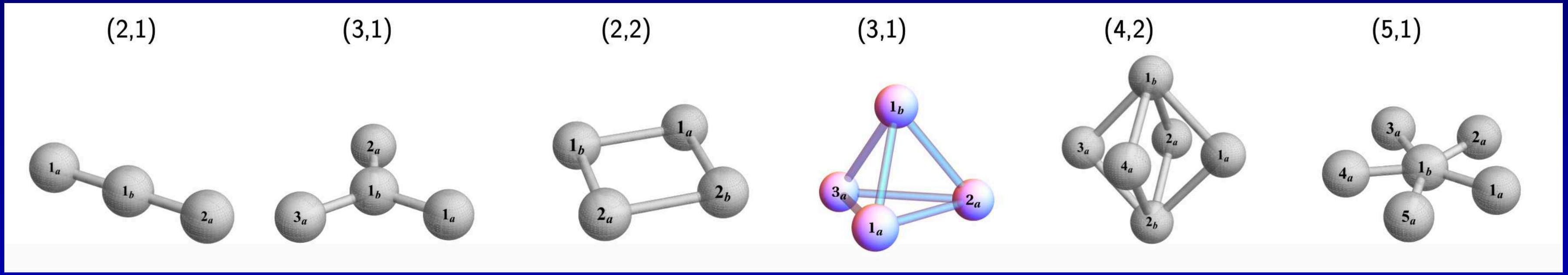

Next sections: applications of $(2,2)$-sites and $(3,1)$-sites in a tetrahedral geometry

3-Application: 4-sites in a ring: Protocol designs for NOON states

What is a NOON state?

- Definition: It is an *all and nothing* superposition of two different modes. For N particles, it has the form:

$$|\mathrm{NOON}\rangle = \frac{1}{\sqrt{2}}\left(|N,0\rangle + e^{i\varphi}|0,N\rangle\right)$$

where the phase φ typically records information in applications

- Applications:
  Quantum metrology and sensing
  Quantum lithography
  Quantum communication
  Quantum computing
  ......

Curiosity: NOON state in arts

Work by Jonas Wood - State I (NOON)

- *Here we show how to generate a NOON state and, in additon, how to encode a phase into this NOON state.*

- *Our approach is based on the formation of an uber-NOON state en route to the final NOON state.*

Uber-NOON state:

- Consider a closed-circuit of 4 sites, with a Fock-state input $|\Psi_0\rangle = |M, P, 0, 0\rangle$. The initial step is to create an *uber-NOON state*, with the general form:

$$|\text{u-NOON}\rangle = \frac{1}{2}\big(|M, P, 0, 0\rangle + e^{i\varphi_1}|M, 0, 0, P\rangle + e^{i\varphi_2}|0, P, M, 0\rangle + e^{i\varphi_3}|0, 0, M, P\rangle\big)$$

for a set of phases $\{\varphi_1, \varphi_2, \varphi_3\}$. It may be viewed as an embedding of NOON states within two-site subsystems

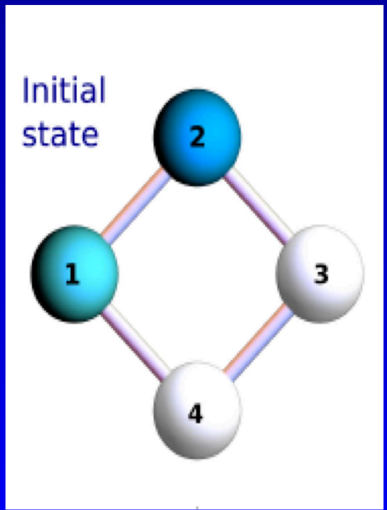

- *We then describe two protocols to extract a NOON state from an uber-NOON state.*
- *For this, we consider a model of dipolar bosons confined to 4 wells, more especifically, to a closed circuit of 4 sites.*
- *The system has long-range interactions and can be described by the EBHM.*

Extended 4-site Bose-Hubbard Model (EBHM)

$$H = \frac{U_0}{2}\sum_{i=1}^{4} N_i(N_i - 1) + \sum_{i=1}^{4}\sum_{j=1, j\neq i}^{4} \frac{U_{ij}}{2} N_i N_j - \frac{J}{2}\left[(a_1^\dagger + a_3^\dagger)(a_2 + a_4) + (a_1 + a_3)(a_2^\dagger + a_4^\dagger)\right],$$

- U_0: characterizes the interaction between bosons at the same site
- $U_{ij} = U_{ji}, i \neq j$: characterize DDI between bosons at different sites (i and j)
- J: couplings for the tunneling between different sites
- Integrability condition:

  The integrable closed 4-wells model can be obtained from EBHM if:

$$U_0 = U_{13} = U_{24}, \quad U_{12} = U_{23} = U_{34} = U_{14}.$$

- Conserved quantities:

The model has 4 modes, so 4 independent conserved quantities are expected:

$$[H, N] = [H, Q_k] = [N, Q_k] = [Q_1, Q_2] = 0, \ {\scriptstyle k=1,2.}$$

$$Q_1 = \frac{1}{2}(N_1 + N_3 - a_1^\dagger a_3 - a_3^\dagger a_1),$$
$$Q_2 = \frac{1}{2}(N_2 + N_4 - a_2^\dagger a_4 - a_4^\dagger a_2),$$

Hereafter we consider the integrable EBHM case.

To generate NOON states we consider that:

- the system is initially in a Fock state $|\Psi_0\rangle = |M, P, 0, 0\rangle$,

  with total boson number $N = M + P$ odd

- the system is in the resonant tunneling regime

  achieved when $U|M - P| \gg J$, where $U = (U_{12} - U_0)/4$.

  In this resonant regime:

  a) the energy levels separate into distinct bands

  b) an effective Hamiltonian H_{eff}, dynamically equivalent to the integrable EBHM, can be obtained

  c) H_{eff} can be written in terms of charges Q_1, Q_2

  d) H_{eff} enables the derivation of analytical expressions for physical quantities.

Significant feature:

- Under this H_{eff}, the time evolution of:
  $N_1 + N_3 = M$ is constant
  $N_2 + N_4 = P$ is constant

- In this resonant tunneling regime:
  M particles can oscillate between sites $1, 3$: subsystem A
  P particles can oscillate between sites $2, 4$: subsystem B

NOON-state protocols:

- We describe two protocols that enable the generation of NOON states. For Protocol I the outcomes are probabilistic while Protocol II are deterministic.

- Both protocols consider the initial state $|\Psi_0\rangle = |M, P, 0, 0\rangle$ and are built around a general time evolution operator:

$$\mathcal{U}(t,\mu,\nu) = \exp\left(-\frac{it}{\hbar}[H + \mu(N_2 - N_4) + \nu(N_1 - N_3)]\right)$$

The applied field strengths μ, ν implement the breaking of integrability

NOON-state protocols: times

We consider three time intervals: $t_{\rm m}$, t_μ and t_ν

- t_m: corresponding to integrable time evolution, is associated with evolution to a particular uber-NOON state.

  It is given by $t_{\rm m} = \pi/(2\Omega)$,

  with $\Omega = J^2/(4U((M-P)^2-1))$ and $U = (U_{12} - U_0)/4$

- t_μ and t_ν: associated with smaller scale non-integrable evolution (implemented by the external fields μ, ν); produce phase encoding.

  It is convenient to introduce the phase variable $\theta = 2\mu t_\mu/\hbar$,

  and to fix $t_\nu = \hbar\pi/(4M\nu)$.

NOON state generation scheme:

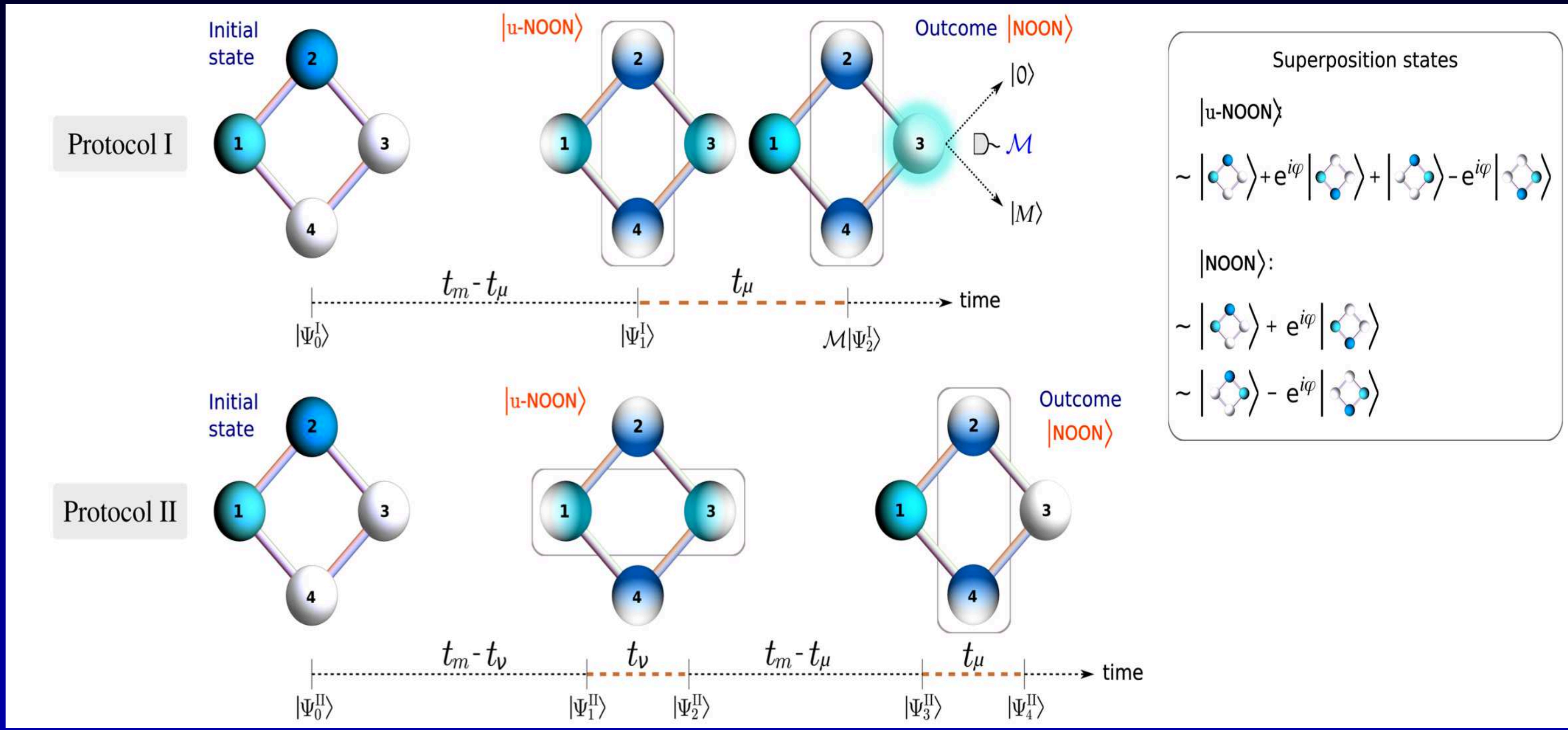

The four spheres on the left represent the initial state, with white indicating empty site and cyan and blue M and P particles, respectively. Gradient colors are used to indicate that the state of a site is entangled with the rest of the system - superposition states for each step are shown in the framed legend. Rectangles represent applied external fields to sites 1-3 (ν) and 2-4 (μ).

Protocol I:

Here are the steps we implement to arrive at a NOON state in subsystem $B = \{2, 4\}$:

$$\text{(i)} \quad |\Psi_1^{\mathrm{I}}\rangle = \mathcal{U}(t_{\mathrm{m}} - t_\mu, 0, 0)\, |\Psi_0\rangle$$

$$\text{(ii)} \quad |\Psi_2^{\mathrm{I}}\rangle = \mathcal{U}(t_\mu, \mu, 0)\, |\Psi_1^{\mathrm{I}}\rangle$$

$$\text{(iii)} \quad |\Psi_3^{\mathrm{I}}\rangle = \mathcal{M}\, |\Psi_2^{\mathrm{I}}\rangle$$

We let the system evolve during a time $t_{\mathrm{m}} - t_\mu$ (integrable evolution), then we apply a field μ across sites $2 - 4$ during a very short time t_μ. Finally we measure the number of bosons at site 3. This produces a high-fidelity NOON state across sites $2 - 4$ (subsystem B)

Protocol I:

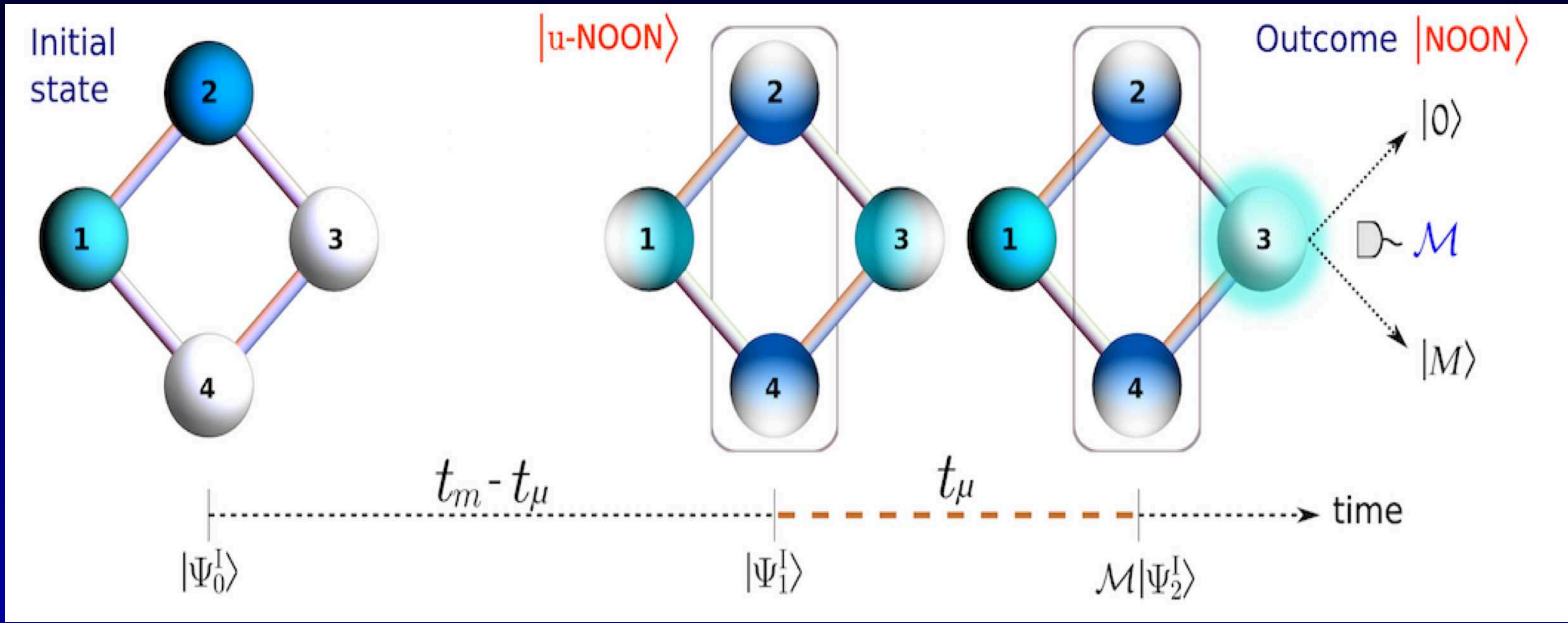

In Protocol I the system evolves for $t_{\mathrm{m}} - t_\mu$, towards the u-NOON state. Then, a field is applied across sites 2-4 for time t_μ, to encode a phase. The cyan halo portrays a measurement process at site 3: outcomes $|0\rangle$ and $|M\rangle$ signify which of two possible NOON states results across sites 2-4.

Analytical results:

Analytic results are obtained by employing the effective Hamiltonian in an extreme limit, with divergent applied fields acting for infinitesimally small times: $\mu \to \infty, t_\mu \to 0$, such that θ remains finite. Here $\beta = (-1)^{(N+1)/2}$. We find for the final state at step (iii):

$$|\Psi_3^{\mathrm{I}}\rangle = \begin{cases} \dfrac{1}{\sqrt{2}} \left(\beta\,|M, P, 0, 0\rangle + e^{iP\theta}\,|M, 0, 0, P\rangle\right), \; r = 0 \\ \dfrac{1}{\sqrt{2}} \left(|0, P, M, 0\rangle - \beta e^{iP\theta}\,|0, 0, M, P\rangle\right), \; r = M \end{cases}$$

- These states are recognized as products of a NOON state for subsystem $B = \{2, 4\}$ with Fock basis states for subsystem $A = \{1, 3\}$.

Protocol II:

Here the following steps are implemented to arrive at a NOON state in subsystem $B = \{2, 4\}$:

$$\text{(i)} \quad |\Psi_1^{\text{II}}\rangle = \mathcal{U}(t_{\text{m}} - t_\nu, 0, 0)\, |\Psi_0\rangle$$

$$\text{(ii)} \quad |\Psi_2^{\text{II}}\rangle = \mathcal{U}(t_\nu, 0, \nu)\, |\Psi_1^{\text{II}}\rangle$$

$$\text{(iii)} \quad |\Psi_3^{\text{II}}\rangle = \mathcal{U}(t_{\text{m}} - t_\mu, 0, 0)\, |\Psi_2^{\text{II}}\rangle$$

$$\text{(iv)} \quad |\Psi_4^{\text{II}}\rangle = \mathcal{U}(t_\mu, \mu, 0)\, |\Psi_3^{\text{II}}\rangle$$

The system first evolves for time $t_{\text{m}} - t_\nu$, then a field is applied to sites $1 - 3$ for time t_ν to implement the phase $\pi/2$. Next, the system evolves for time $t_{\text{m}} - t_\mu$, after which a field is applied to sites $2 - 4$ to encode a phase during time t_μ. This results in a NOON state across sites $2 - 4$

Protocol II:

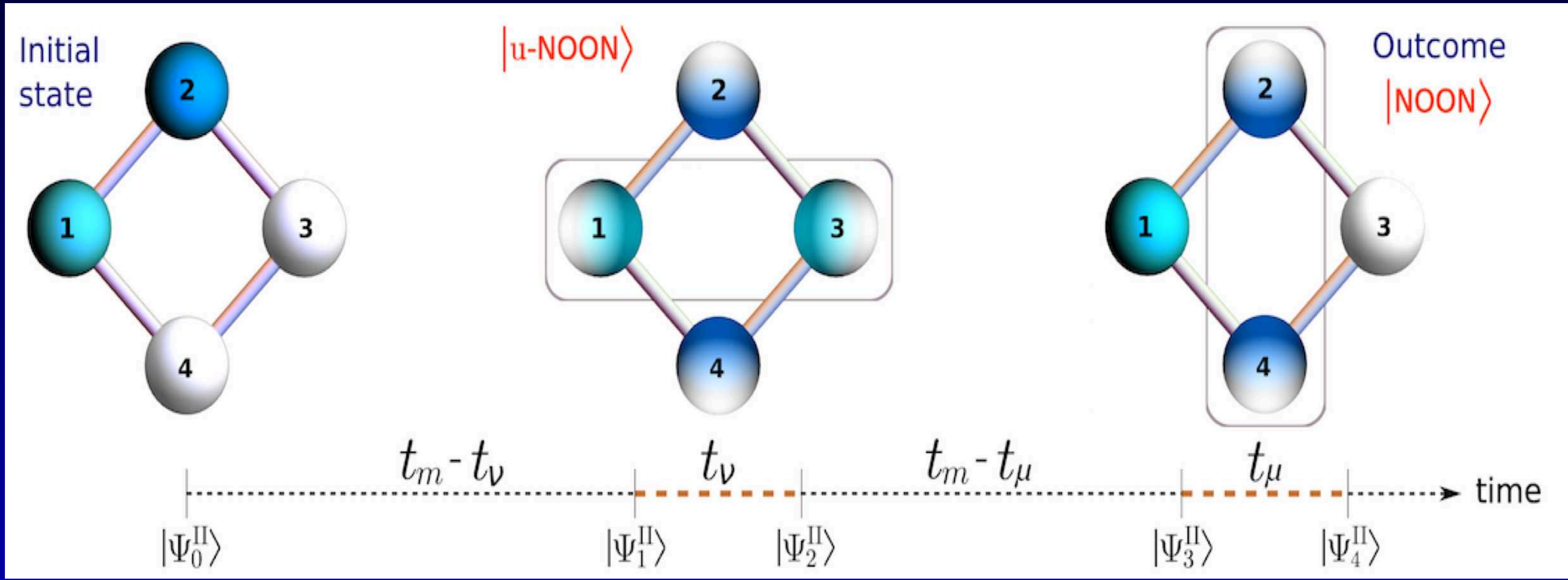

In Protocol II the system first evolves for time $t_{\mathrm{m}} - t_\nu$, then a field is applied to sites 1-3 for time t_ν to implement the phase $\pi/2$. Next, the system evolves for time $t_{\mathrm{m}} - t_\mu$, after which a field is applied to sites 2-4 to encode a phase during time t_μ. This results in a NOON state across sites 2-4, without performing a measurement procedure

Analytic results:

Similar to Protocol I, analytic results are obtained by employing the effective Hamiltonian. We obtain for the final state at step (iv): (here $\Upsilon = \beta \exp(i(P\theta - \pi/2))$)

$$|\Psi_4^{\mathrm{II}}\rangle = \frac{1}{\sqrt{2}}\Big(|M, P, 0, 0\rangle + \Upsilon \, |M, 0, 0, P\rangle \Big)$$

This state is recognized as a product of a NOON state for subsystem $B = \{2, 4\}$ with a deterministic state (Fock basis state) for subsystem $A = \{1, 3\}$.

Protocol fidelities:

- We give numerical simulations of the protocols to show that, for physically realistic settings (see Set I and Set II) high-fidelity outcomes for NOON state production persist.

- The fidelities of Protocols I and II are defined as:

$$F_{\mathrm{I}} = |\, \langle \Psi_3^{\mathrm{I}} | \Phi_3^{\mathrm{I}} \rangle \,| \qquad F_{\mathrm{II}} = |\, \langle \Psi_4^{\mathrm{II}} | \Phi_4^{\mathrm{II}} \rangle \,|$$

$|\Psi\rangle$: denotes the analytical states obtained using the effective Hamiltonian

$|\Phi\rangle$: denotes the numerically calculated state obtained by EBHM time evolution.

OBS: The fidelities are computed for $P\theta$ ranging from 0 to π, achieved by varying t_μ. As the values remain almost constant for $P\theta \in [0, \pi]$, varying less than 1%, we display here only one case.

Protocol fidelities:

	$F_{\mathbf{I}}$		$F_{\mathbf{II}}$	$P\theta = \pi/2$		
	$r = 0$	$r = M$		t_μ	t_ν	t_m
Set 1	0.986	0.997	0.974	0.0024 s	0.0065 s	6.1639 s
Set 2	0.964	0.991	0.920	0.0026 s	0.0072 s	2.8913 s

Fidelities for Protocols I (F_{I}) and II (F_{II}) and related times t_m, t_μ and t_ν (fixed), concerning to the parameters of Set 1 and Set 2, for $|\Psi_0\rangle = |4, 11, 0, 0\rangle$.

- Two realistic sets of parameters (in Hz):
  Set 1: $\{U/\hbar = 104.85,\ J/\hbar = 71.62,\ \mu/\hbar = 30.02\}$
  Set 2: $\{U/\hbar = 105.60,\ J/\hbar = 104.95,\ \mu/\hbar = 27.42\}$

Observations:

- Both protocols display high fidelity results greater than 0.9.
- The higher fidelity results associated to parameter Set 1, compared to Set 2, are produced through longer evolution time: these results reflect the trade-off between fidelity and total evolution time.
- The required times $tm, 2tm$ to produce the NOON states are comparable with typical lifetimes of optical lattice traps.
- Advantage of the protocols: the evolution time is independent of total particle number, offering an encouraging prospect for scalability.

Readout statistics:

- We can test the reliability of the system through a statistical analysis of local measurement outcomes.
- To do this, for both protocols, once the output state has been attained, we can continue to let the system evolve during a time t_m.
- This yields the readout states that can be obtained analitically using the effective Hamiltonian in the idealized limit, and also numerically using the EBHM.
- Then we can find the readout probabilities that we present here for both Protocols for the Set I.

Readout probabilities:

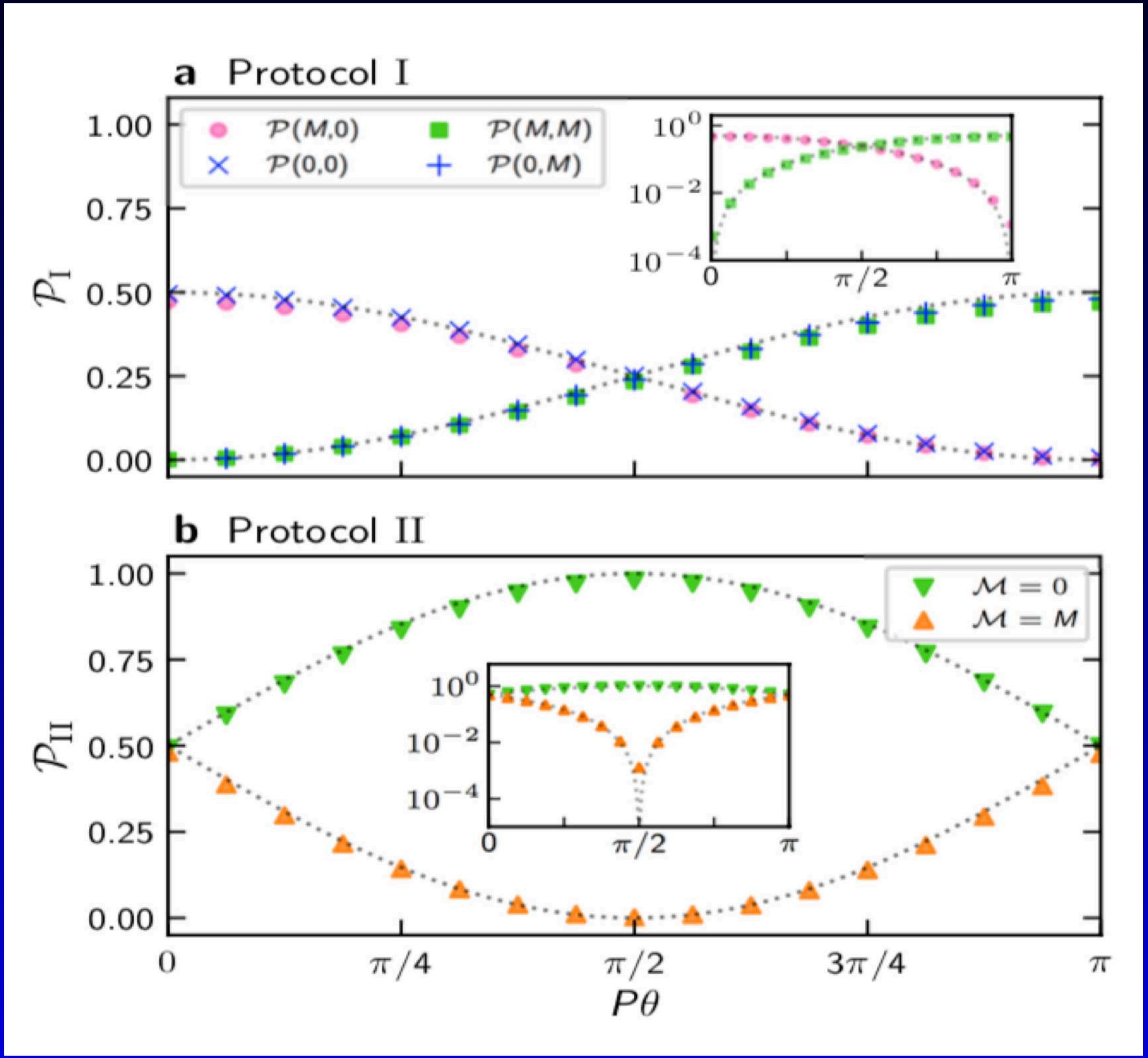

Readout probabilities for Protocols I and II. Comparison between analytic (dotted lines) and numerically (colored symbols) calculated probabilities for parameters of Set 1 for different values of $P\theta$. A good agreement is found.

Experimental feasibility:

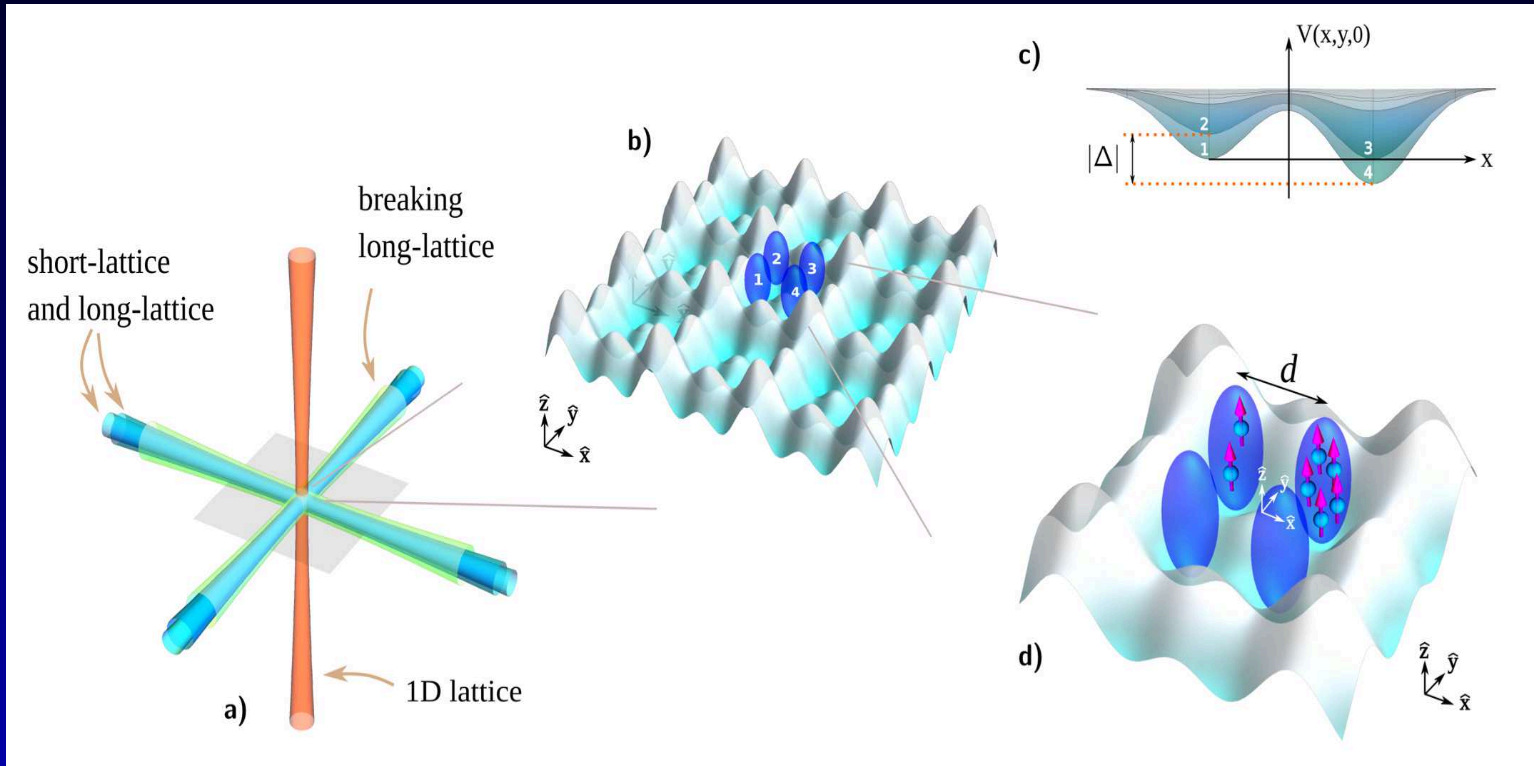

a) Trapping scheme: 2D square optical lattice is generated with 2 sets of counterpropagating laser beams crossing at 90. The superlattice of 4-site model is achieved overlapping the 2D short lattice (cyan) and long-lattice (blue). The vertical lattice (orange) provides confinement in z direction. An additional 2D square long-lattice (green) is used to implement the integrability break control. b) Zoom into the region of the superlattice which contains the 4-site plaquette. c) Breaking-of-integrability scheme

4-Application: 4-sites in a tetrahedral geometry: Quantum Turntable

- *Here we design a quantum turntable that spatially transfers entangled states with high fidelity in a rotating frame.*

- For this, we study a system of ultracold dipolar atoms in a tetrahedral geometry, that is set to rotate at constant angular frequency Ω.

- The system can be described by the Extended Bose-Hubbard Model in a rotating frame.

Geometric representation of rotating tetrahedral system

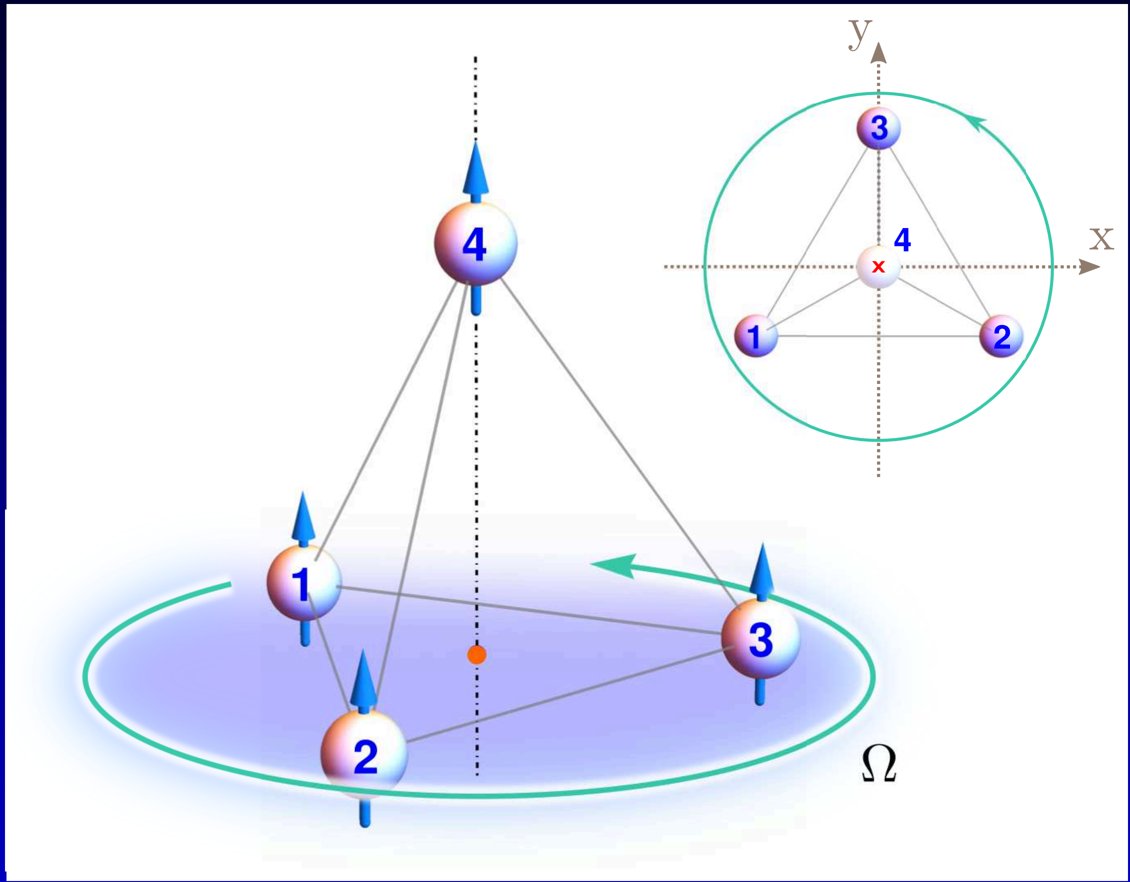

Sites 1, 2, 3 form the triangular base. Blue arrows show dipoles along z-axis. The system rotates around z with angular freq. Ω.

Extended Bose-Hubbard model in a rotating frame:

$$\mathcal{H} = \frac{U_0}{2}\sum_{i=1}^{4} N_i(N_i - 1) + \sum_{i=1}^{4}\sum_{j=1;j\neq i}^{4} \frac{U_{ij}}{2} N_i N_j$$

$$- J \sum_{i<j=1}^{4} (a_i^{\dagger} a_j + a_j^{\dagger} a_i) + \mathcal{H}_{\mathrm{rot}}$$

- U_0: characterizes the interaction between bosons at the same site
- $U_{ij} = U_{ji}, i \neq j$: characterize DDI between bosons at different sites (i and j)
- J: couplings for the tunneling between different sites
- $\mathcal{H}_{\mathrm{rot}}$: characterizes the rotation of the system.

Our approach combines various ingredients:

- *Long-range interactions via dipolar atoms.*
- *Non-equilibrium phenomena via use of a rotating frame.*
- *Property of superintegrability guiding the proposal.*

Cases Considered:

- Non-rotating case: *Superintegrable.*
- Rotating case: *Integrability persists.*

  Bethe Ansatz applied as analytical basis for the quantum turntable.

Superintegrability in a Static Frame ($H_{\text{rot}} = 0$)

- Geometric symmetry: $U_{14} = U_{24} = U_{34}$, $U_{12} = U_{23} = U_{13}$
- Superintegrability condition: $U_{12} = U_0 = 2U$
- $\mathcal{H}$ reduces to: $\mathcal{H} = \mathcal{H}_0 = U(N_1 + N_2 + N_3 - N_4)^2 - J\sum_{i<j}(a_i^\dagger a_j + a_j^\dagger a_i)$

◇ It has 4 degrees of freedom.

◇ It is superintegrable: has more conserved quantities (5) than degrees of freedom (4).

Then the system is set to rotate.

Integrability in a Rotating Frame:

- Rotation term: $H_{\rm rot} = -\zeta \mathcal{J}$

$$\mathcal{J} = i\sqrt{3}\Big[(a_2^\dagger a_1 + a_3^\dagger a_2 + a_1^\dagger a_3) - (a_1^\dagger a_2 + a_3^\dagger a_1 + a_2^\dagger a_3)\Big]$$

- Total Hamiltonian: $\mathcal{H}(\zeta) = \mathcal{H}_0 - \zeta \mathcal{J}$
- Effect: superintegrability is broken, but...
- Integrability preserved: 4 conserved operators.
- These conserved operators can define H_{eff}, enabling the derivation of analytical expressions for physical quantities.

Superintegrability:

- To establish this, define $Q_k = b_k^\dagger b_k$, $k = 1, 2, 3$, where

$$b_k = \frac{1}{\sqrt{3}}(a_1 + \nu_k a_2 + \nu_k^{-1} a_3), \qquad \nu_k = e^{2\pi i(k-1)/3}$$

- In terms of the above operators, the Hamiltonian is

$$\mathcal{H}_0 = U(Q_1 + Q_2 + Q_3 - N_4)^2 - J(2Q_1 - Q_2 - Q_3) - \sqrt{3}J(b_1^\dagger a_4 + a_4^\dagger b_1). \quad (3)$$

- satisfying

$$[\mathcal{H}_0, N] = 0, \quad [\mathcal{H}_0, Q_2] = 0, \quad [\mathcal{H}_0, Q_3] = 0,$$
$$[Q_2, Q_3] = 0, \quad [N, Q_2] = 0, \quad [N, Q_3] = 0.$$

Superintegrability:

- Next, the Jordan-Schwinger rep. of $sl(2)$ provides:

$$
\begin{aligned}
\mathcal{J}_1 &= \frac{1}{2}(b_2^\dagger b_3 + b_3^\dagger b_2), \\
\mathcal{J}_2 &= \frac{1}{2} b_2^\dagger b_3 - b_3^\dagger b_2), \\
\mathcal{J}_3 &= \frac{1}{2}(Q_3 - Q_2),
\end{aligned}
$$

- satisfying $[\mathcal{J}_j, \mathcal{J}_k] = i \sum_l \epsilon_{jkl} \mathcal{J}_l$, where ϵ_{jkl} is the Levi-Civita symbol. Moreover, the relation $[Q_2 + Q_3, \mathcal{J}_j] = 0$ holds.

- In addition to $\{\mathcal{H}_0, N, Q_2, Q_3\}$, there are two additional conserved quantities:

$$[\mathcal{H}_0, \mathcal{J}_1] = 0, \quad [\mathcal{H}_0, \mathcal{J}_2] = 0.$$

Superintegrability:

- Due to the relation

$$\mathcal{J}_1\mathcal{J}_2 - \mathcal{J}_2\mathcal{J}_1 = \frac{i}{2}(Q_3 - Q_2)$$

- we may choose the following set of *five algebraically independent* conserved operators

$$\{\mathcal{H}_0,\ N,\ Q_2 + Q_3,\ \mathcal{J}_1,\ \mathcal{J}_2\}$$

for the system, *establishing superintegrability.*

Breaking superintegrability in a rotating frame:

- Total Hamiltonian: $\mathcal{H}(\zeta) = \mathcal{H}_0 - \zeta \mathcal{J}$

  $\rightarrow$ *energy levels shown in the next figure*

- In the rotating frame, the additional operators $\mathcal{J}_1$ and $\mathcal{J}_2$ are no longer conserved, since: *(due to $\mathcal{J} = 2\mathcal{J}_3$.)*

$$[\mathcal{H}(\zeta), \mathcal{J}_1] = -2i\zeta\mathcal{J}_2, \qquad [\mathcal{H}(\zeta), \mathcal{J}_2] = 2i\zeta\mathcal{J}_1 \tag{4}$$

- But 4 mutually commuting conserved operators remain:

$$\{\mathcal{H}(\zeta),\, N,\, Q_2,\, Q_3\}$$

  ensuring integrability of the rotating system.

Energy spectrum:

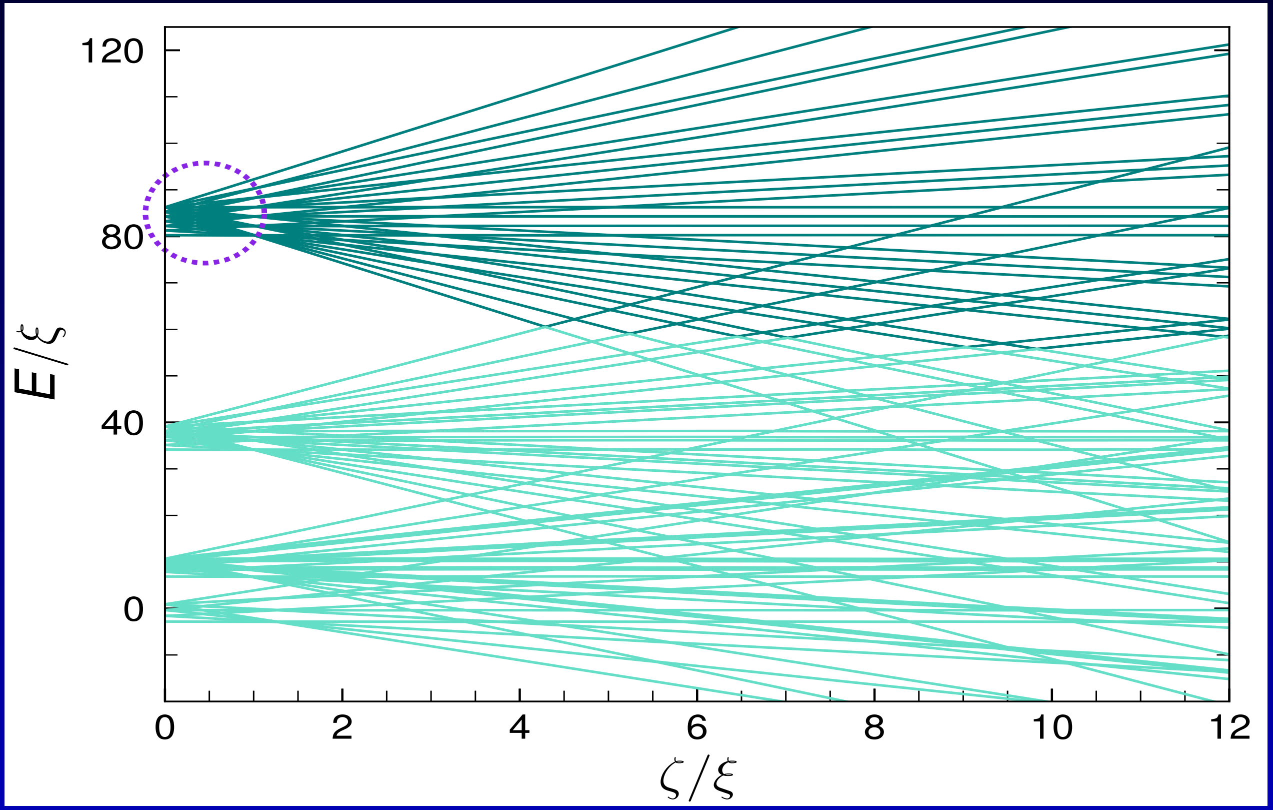

Dimensionless energy levels for the total Hamiltonian $\mathcal{H}(\zeta)$ as a function of ζ/ξ for $N = 6$. Parameters are $U/\hbar = 2\pi \times 2.16$ Hz and $J/\hbar = 2\pi \times 0.31$ Hz, for dysprosium ^{164}Dy. Top band (blue) shows associated states with expectation value $\langle N_4 \rangle \approx 0$ or 6. Circle marks region enlarged in next fig.

Energy spectrum:

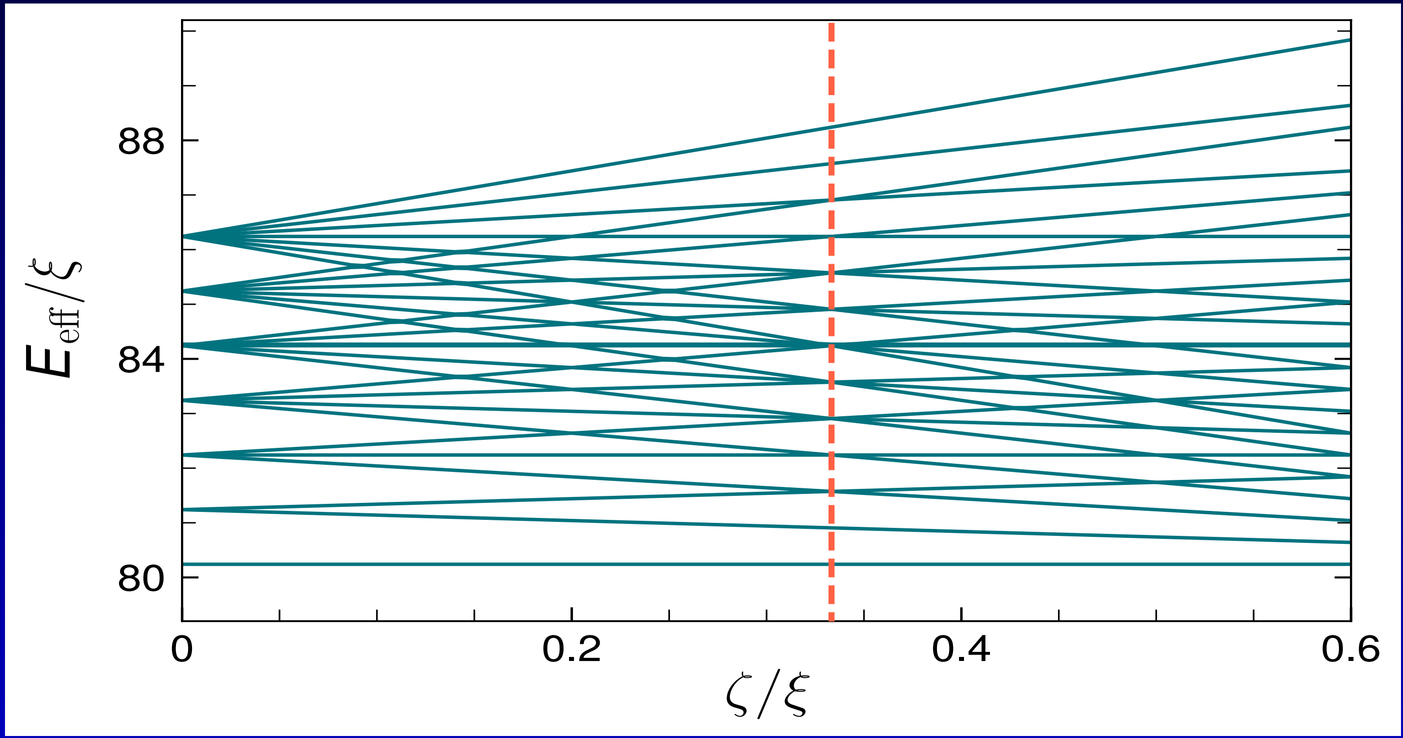

The distinctive character of uniformly-spaced, degenerate energy levels is observable at:

- $\zeta/\xi = 0$
- $\zeta/\xi = 1/3$ (orange line) $\rightarrow$ We use here this case.

Expectation values of populations:

- Expectation values of populations at sites $k = 1, 2, 3$

$$\langle N_k \rangle = \sum_{i=1}^{3} \frac{n_i}{9} \Big\{ 1 + 4 \cos\theta_{k,i}(t) [\cos(\xi t) + \cos\theta_{k,i}(t)] \Big\},$$

where $\theta_{k,i}(t) = t\zeta + 2\pi(k-i)/3$

$$\xi = 3J - \tfrac{3J\gamma}{2} \left[\tfrac{N+1-\gamma}{(N-2n_4-\gamma)^2-1} \right], \quad \gamma = \tfrac{J}{2U}.$$

- At $\zeta = \xi/3$, this eq. yields the time interval required for particle transfer between consecutive sites:

$$\tau = \pi/\xi$$

Expectation values of populations:

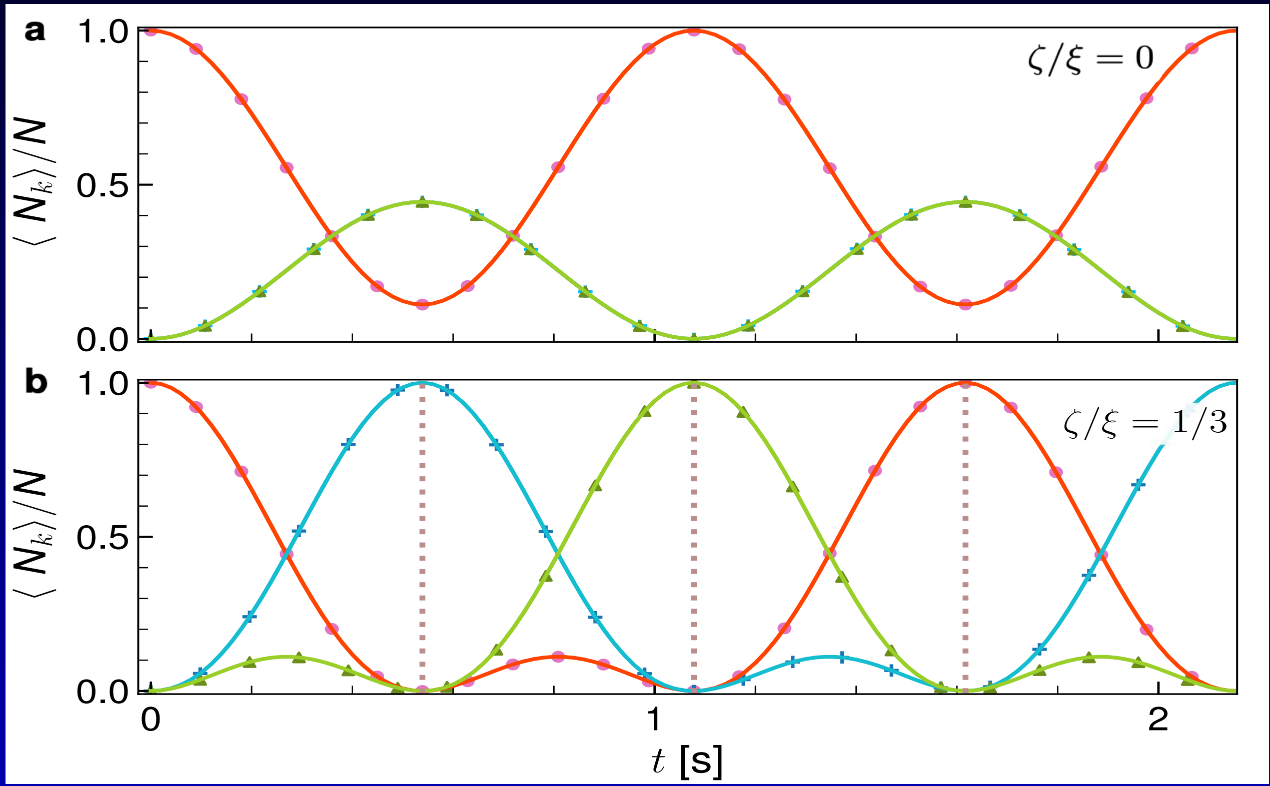

- Comparison between numerical simulation (markers) and analytical expressions (solid lines) for fractional populations $\langle N_1 \rangle / N$ (red), $\langle N_2 \rangle / N$ (blue) and $\langle N_3 \rangle / N$ (green).
- We consider initial state $|\Psi(0)\rangle = |19, 0, 0, 0\rangle$ and $U/\hbar = 2\pi \times 2.16$Hz, $J/\hbar = 2\pi \times 0.31$Hz. Vertical dashed lines represent times $t = \tau$, $t = 2\tau$ and $t = 3\tau$.

Expectation values of populations:

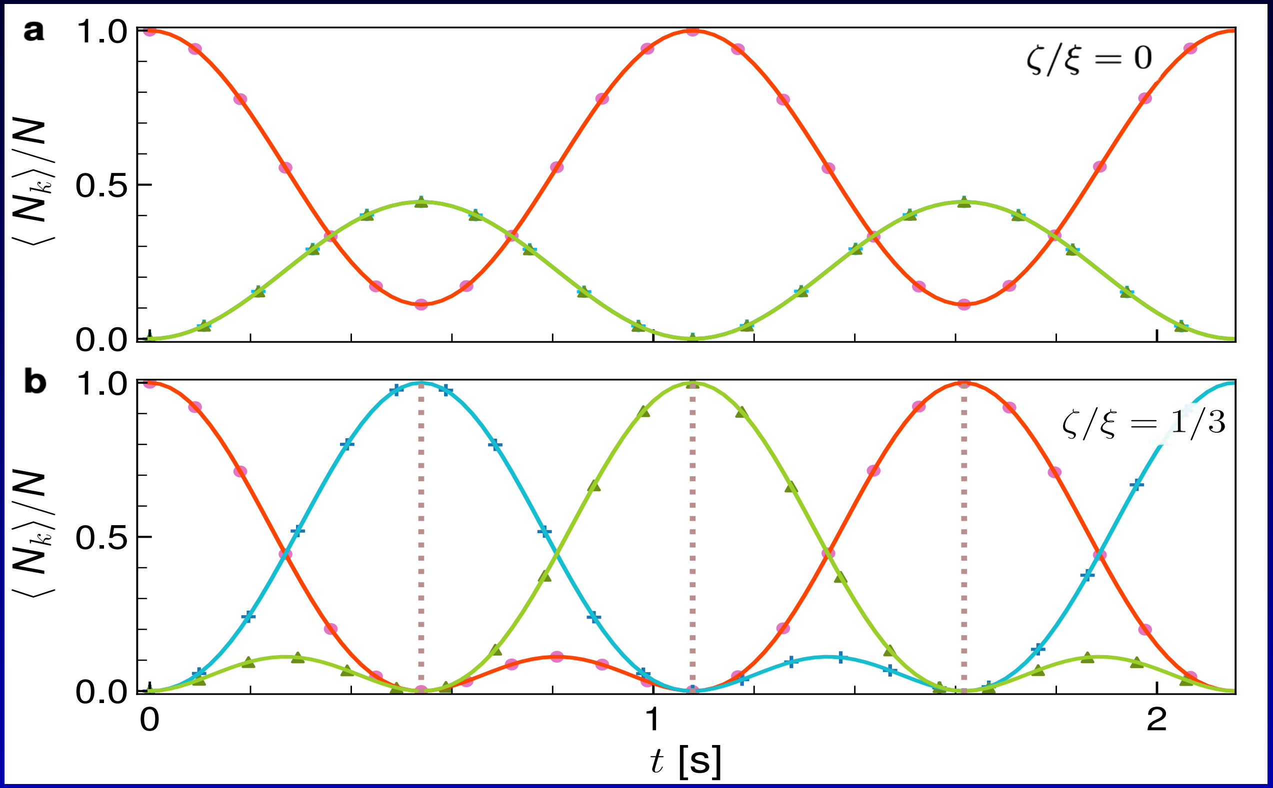

- **a)** Non-rotating case $\zeta = 0$: Expectation of population in site 1 initially decreases over time, splitting equally into sites 2 and 3, returning periodically to attain maximal value.
- **b)** Rotating case $\zeta = \xi/3$: maximal population expectation circulates along sites 1, 2, and 3, in contrast to non-rotating case.

Quantum turntable for different initial states:

The system can act as a quantum turntable, capable of spatially transferring different initial states:

- Fock states
- Entangled states

Transfer of Fock states:

- Schematic of Fock state dynamics on a quantum turntable rotating at Ω. Colored spheres represent sites with particles.

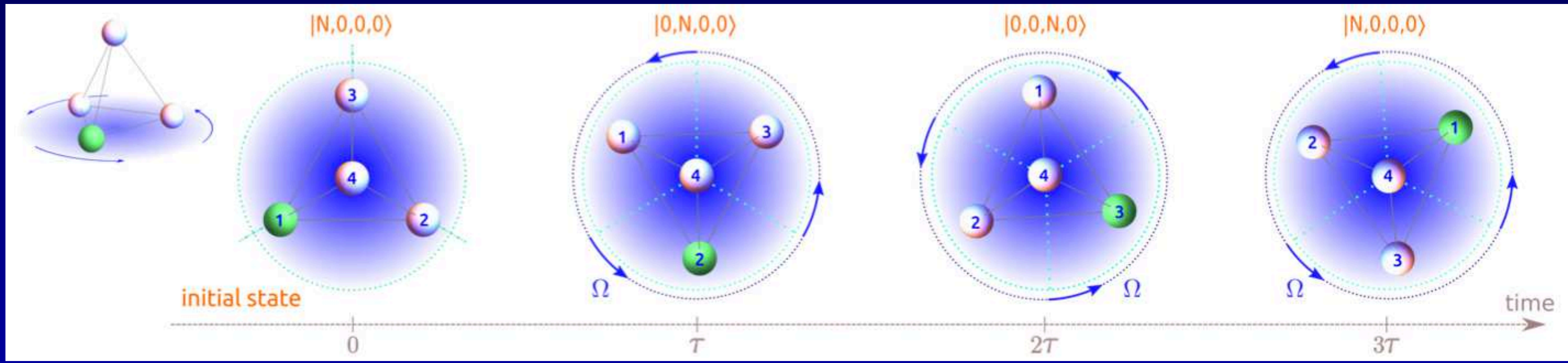

For a particular Ω, the initial state $|N,0,0,0\rangle$ evolves to $|0,N,0,0\rangle$ over time interval τ.

Transfer of NOON states:

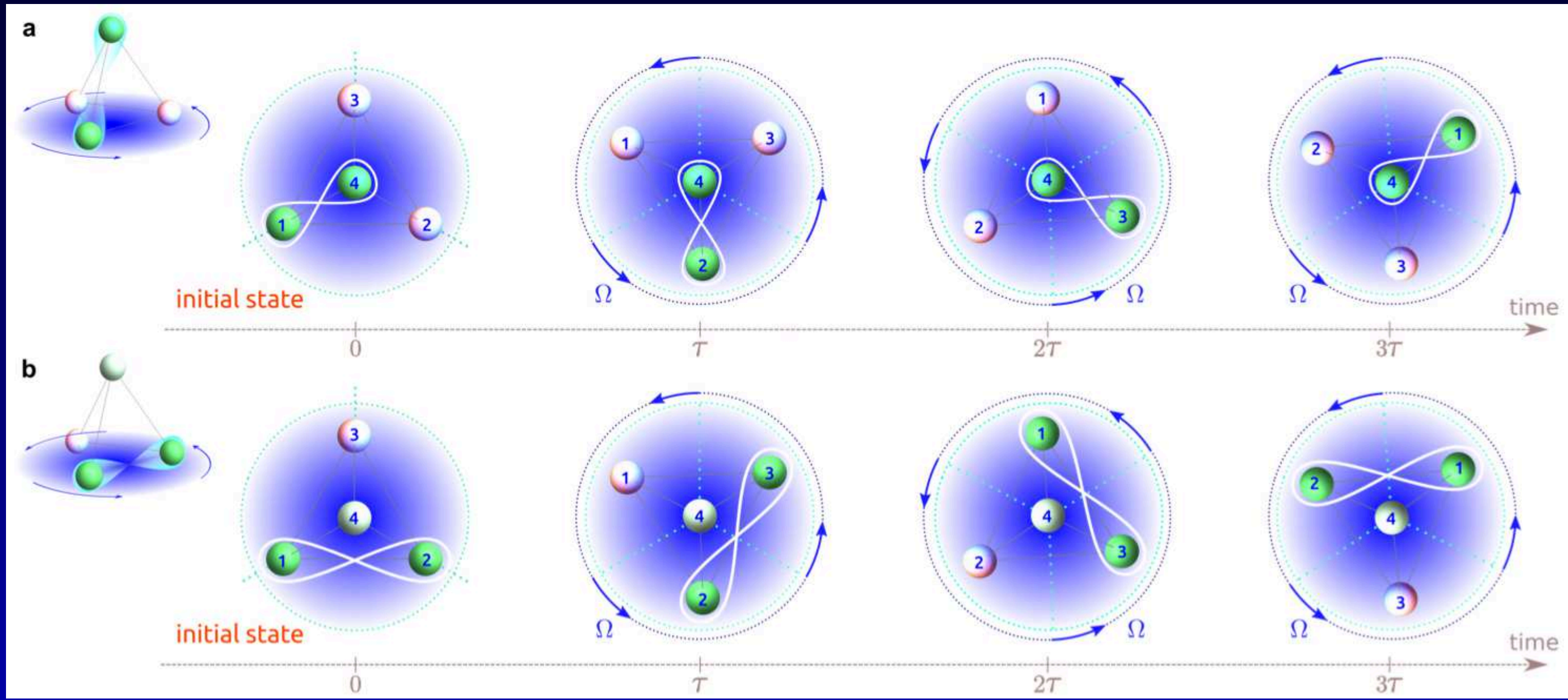

a) One of the components of the NOON state remains fixed at site 4, while the other is transferred across sites 1, 2 and 3.

b) The NOON state prepared in sites 1 and 2 is transferred along the neighbouring two-site subsystems.

Transfer of uber-NOON states:

- Phase shift:
  We identify the occurrence of a phase shift during this operation.

- Quantum sensing potential:
  This result points toward the possibility to implement the turntable as a quantum sensor with supersensitivity.

Fidelity:

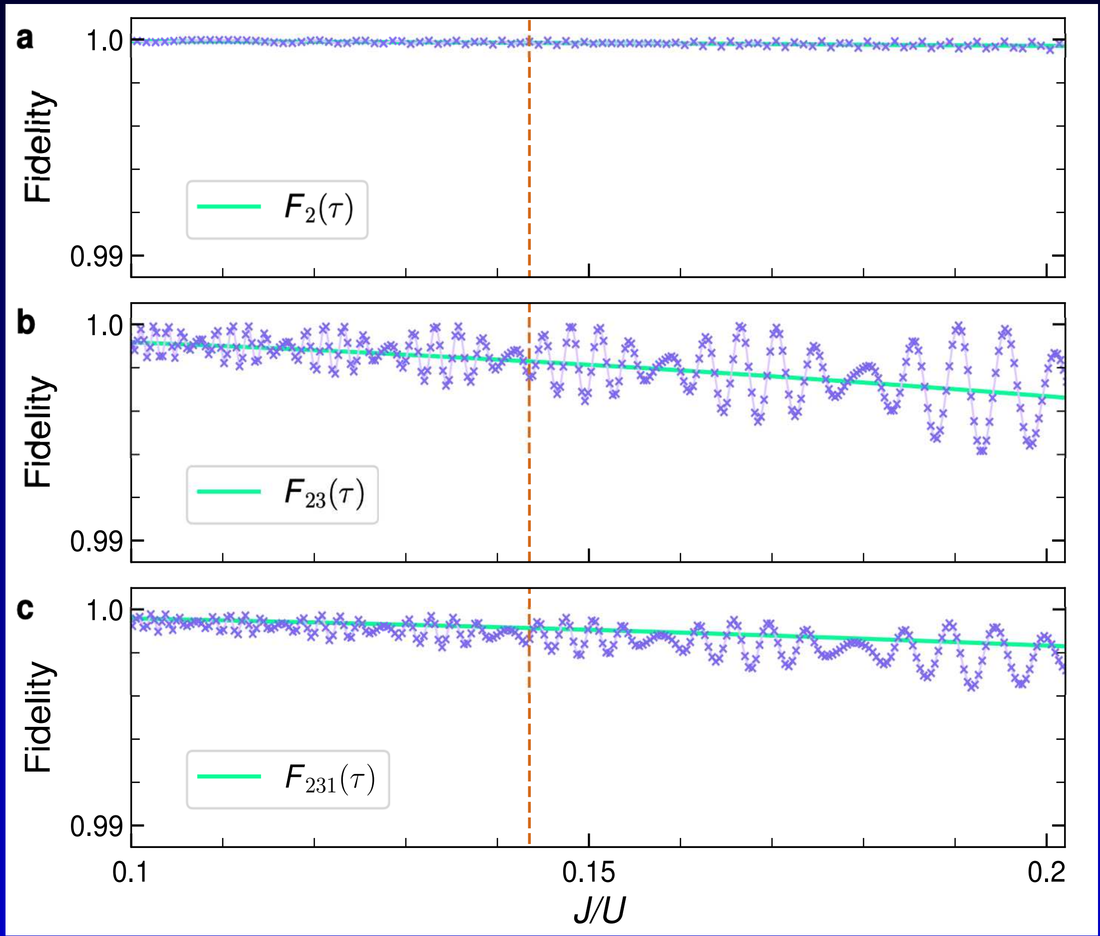

Fidelity computations for N = 19 - numerical versus analytic expressions from Bethe Ansatz results. All cases display high-fidelity results greater than 0.99.

Experimental feasibility:

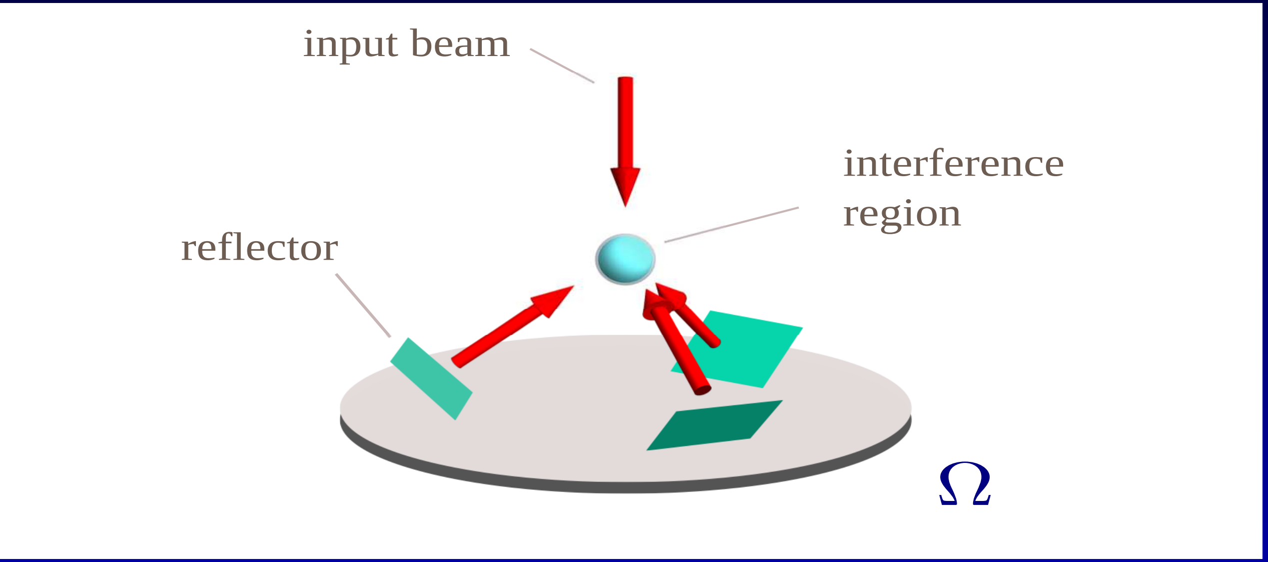

Schematic representation of light interference. A single input laser beam is reflected by a set of reflectors on a rotating platform with a constant angular frequency Ω, generating an optical lattice with tetrahedral geometry in the interference region (cyan sphere).

Newton

Article

High-fidelity transfer of entangled states on a quantum turntable

Graphical abstract

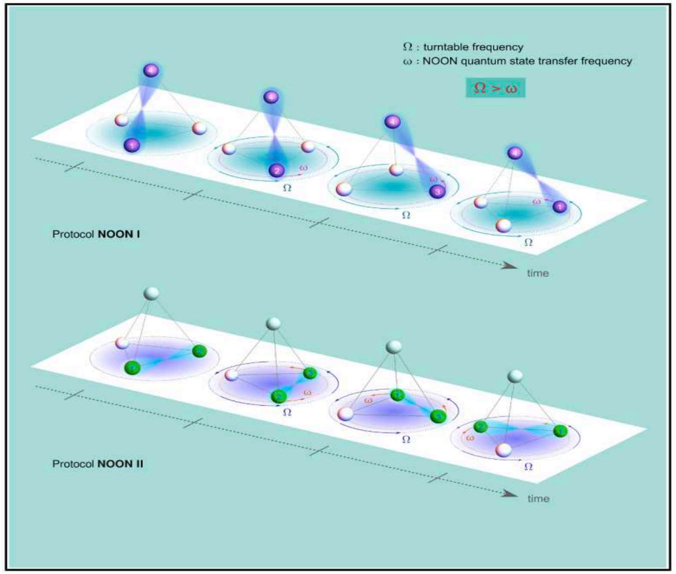

Highlights

- Quantum effects analyzed in a rotating reference frame
- Tetrahedral design based on a superintegrable quantum system
- Frequency of state rotation determined by particle number at a control site
- Entangled states shown to rotate with high fidelity and supersensitivity

Authors

Leandro Hayato Ymai,
Karin Wittmann Wilsmann,
Arlei Prestes Tonel, Angela Foerster,
Jon Links

Correspondence

angela@if.ufrgs.br (A.F.),
jrl@maths.uq.edu.au (J.L.)

In brief

Realizing platforms that can reliably transfer quantum states is key for quantum technologies, and recent efforts have proposed the use of cold atom systems. Ymai et al. design a quantum turntable for the transport of entangled states using a tetrahedral circuit. The performance is quantified through fidelity analyses, and potential applications for quantum sensing are identified. The feasibility of operating the system using ultracold dipolar atoms is also discussed. The results showcase the benefits of superintegrability in the design of supersensitive quantum architectures.

Newton
A Cell Press journal

PREVIEW · Online now, 100258, October 08, 2025 Download Full Issue

Spinning states with a quantum turntable

Philip D. Gregory

Affiliations & Notes Article Info Linked Articles (1)

Download PDF Cite Share Set Alert Get Rights Reprints Previous article Next article

Show Outline

Abstract

The coherent transfer of quantum information between different points in space is challenging. Ymai and Wilsmann et al. show that a spinning tetrahedral arrangement of optical traps realizes a quantum turntable that can coherently transfer the quantum states of magnetic atoms, including entangled states, around the axis of rotation with high fidelity.

Main text

Quantum entanglement is an important tool for developing quantum technologies. The simplest quantum systems encode quantum information into individual particles, or qubits, such that they are independent of each other. On the other hand, more complex systems encode quantum information into many particles which are entangled, meaning that the state of each particle depends upon the state of the others. Entangled states can be engineered using quantum gates, or more generally by engineering interactions between the particles, and are a fundamental component of proposed protocols for quantum computing[1] and quantum sensing.[2] To implement such protocols, precise control over quantum information in many-body systems is required. In particular, controlled and coherent spatial transfer of quantum information is difficult and represents an important experimental and theoretical challenge.

Angela Foerster, Jon Links, and colleagues from the Federal University of Pampa, the Federal University of Rio Grande do Sul, and the University of Queensland theoretically propose a novel technique for the spatial transfer of entangled states of bosons that they refer to as a "quantum turntable,"[3] which they developed for a system of ultracold magnetic atoms. The work gives specific thought to the dysprosium atom (Dy), though should also be relevant to experiments with other magnetic atom species such as chromium and erbium. Such atoms offer long-range and anisotropic interactions due to their large magnetic dipole moments and may be used to study new collective many-body quantum phenomena.[4] For bosonic atoms with large magnetic moments, the collective behavior of the system is described by the extended Bose-Hubbard model,[5] which is the archetypal model for quantum magnetism in systems exhibiting long-range interactions.

Figures (1) Figure Viewer

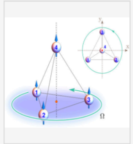

Article metrics

Metric data currently unavailable

Related articles (40)

High-fidelity transfer of entangled states on a quantum turntable
Ymai et al.
Newton, August 22, 2025

Real-time quantum control of spin-coupling damping and application in atomic spin gyroscopes

Prior to the publication, our work was featured in a Preview.
"It highlights and contextualizes significant research."

5- CONCLUSIONS

Conclusions:

- We discussed integrable multi-sites qtum tunneling models, which may be formulated in different configurations and geometries;
- As an application, we showed how to generate and encode a phase into a NOON state by exploring the 4-sites in a ring;
- We showed how to use 4-sites in a tetrahedral geometry to design quantum turntable that spatially transfers entangled states with high fidelity in a rotating frame.

Ongoing/Future work:

- *Compare and contrast the behaviours of open and closed systems, in particular for the 4-wells:*

integrable

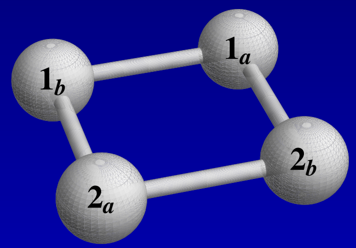

superintegrable

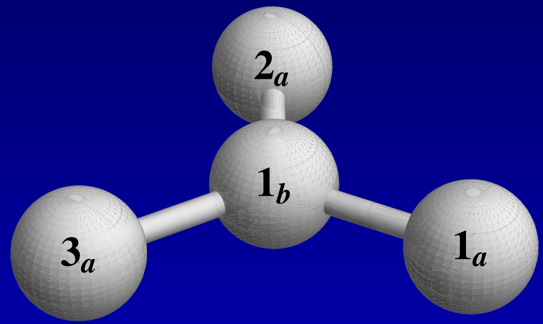

Ongoing/Future work:

- *Design a directional quantum switch:*

  Atoms in well 1 can be transferred to wells 2 or 3

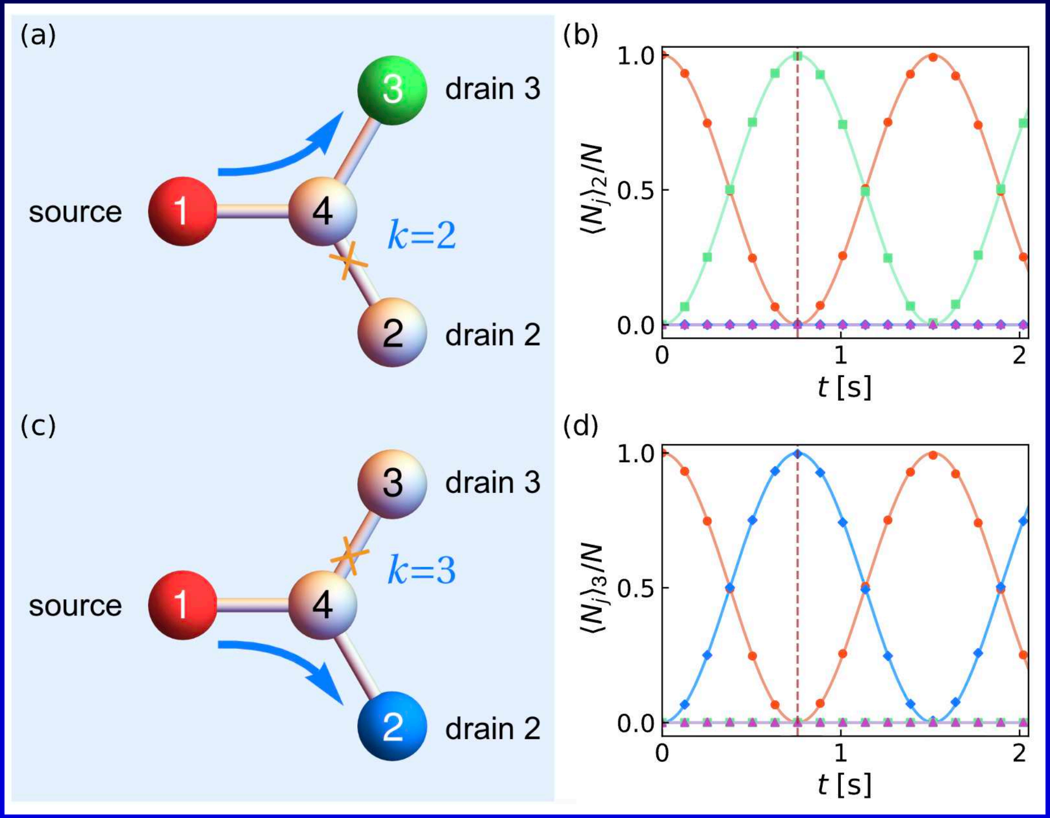

Ongoing/Future work:

- *Design an integrable rotation sensor:*

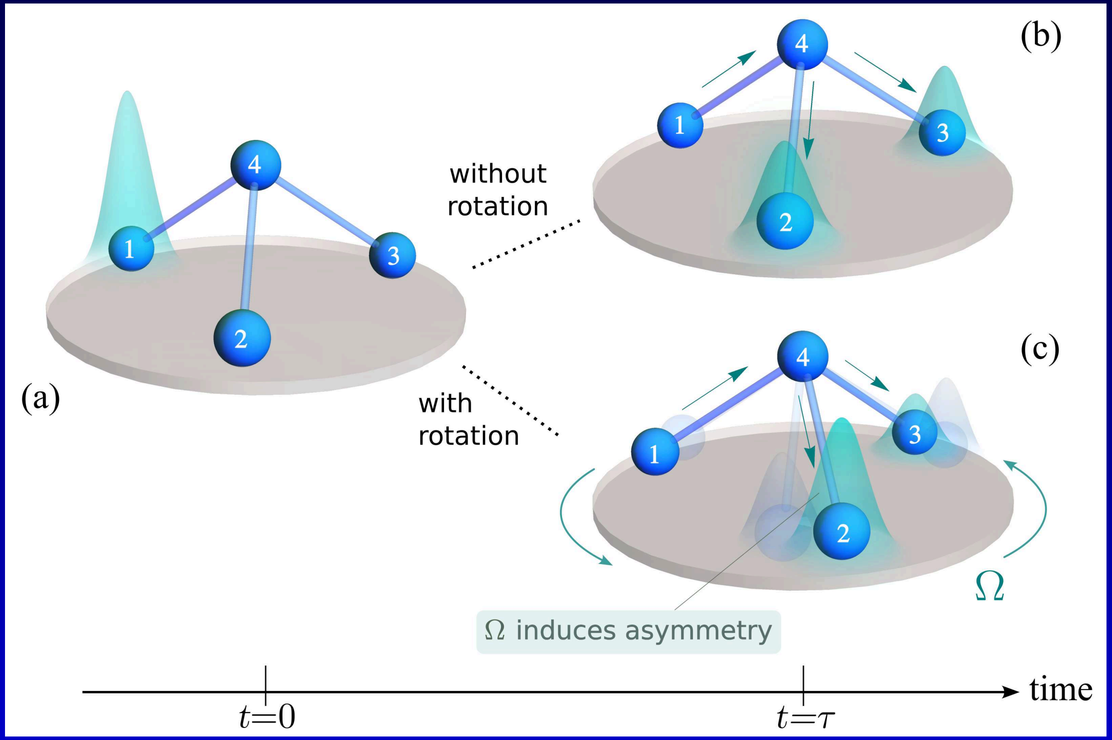

Future work:

- *Extend the techniques to construct more general integrable models, such as tilted 4-site EBHM with nearest-neighbour interactions, and models with higher-order interactions, such as correlated tunneling terms* $N_j a_j^\dagger a_k$;

- *Develop protocols to generate and control other relevant quantum states;*

- *Investigate the possibility of other physical applications for multi-well tunneling models.*

Quantum control designed from broken integrability

- Collaboration:
  University of Queensland

- Main goal:
  Open new avenues in the design and control of quantum architectures using concepts from integrability and its breaking.

- Expected results:
  Promote new opportunities for the construction of atomtronic devices, which are rising as a foundation for new quantum technologies.

Vision for the Future:

We believe the future is quantum, and integrability can offer powerful insights to navigate its complexity!

Collaborators

- Prof. Jon Links, UQ-QLD-Australia
- Prof. Phillip Isaac, UQ-QLD-Australia
- Prof. Arlei Tonel, Unipampa-Brazil
- Prof. Leandro Ymai, Unipampa-Brazil
- Karin Wilsmann (Postdoc), UFRGS-Brazil
- Daniel Grün (Master in 2021, UFRGS-Brazil), Innsbruck
- Bruno Barros, (Master in 2024, UFRGS-Brazil), Canada
- Genessi Sa Neto (Master student), UFRGS-Brazil
- Joel Bacellar Neves (Master student), UFRGS-Brazil
- Mariana Scola (Master student), UFRGS-Brazil
- Pedro Iatauro (Master student), UFRGS-Brazil
- Pedro de Souza (undergraduate student), UFRGS-Brazil
- Pedro de Nega (undergraduate student), UFRGS-Brazil

Team in Porto Alegre:

Photo taken in Porto Alegre, September, 2018

Team in Porto Alegre:

Photo taken in Porto Alegre, June, 2025

THANK YOU !!!

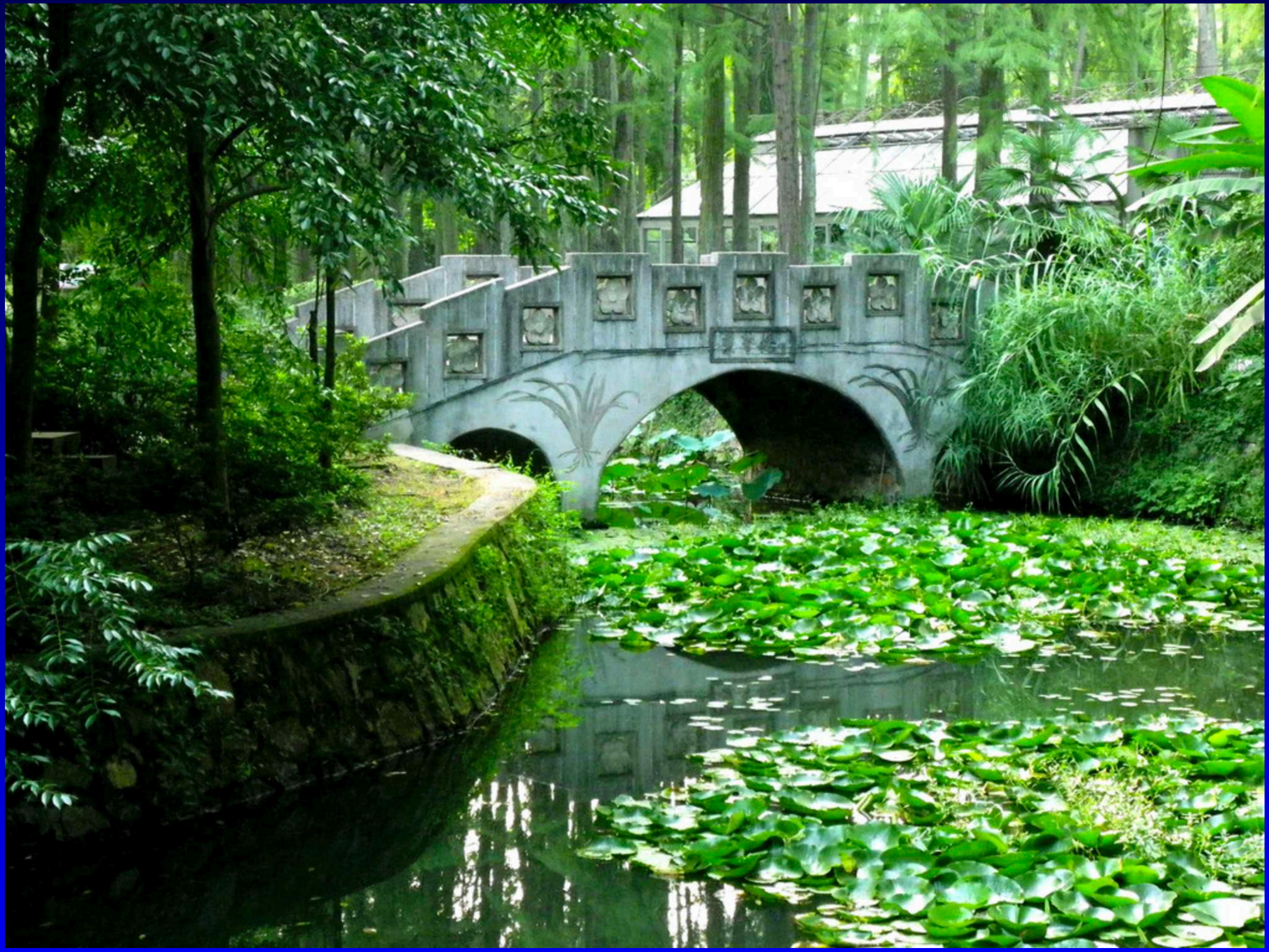

Importance of the NOON states:

- NOON states are entangled, Schrödinger cat states, at the core of many new applications in *Quantum information;*
- NOON states are important in *Quantum metrology and sensing* for their ability to make precision phase measurements when used in an interferometer;
- NOON states can overcome diffraction limits in *Quantum lithography;*
- NOON states are used to test Bell-type inequalities violations in *Fundamental Physics;*
- NOON states are expected to extend to areas such as *Chemistry and Biology*; e.g. improving the resolution of microscopes.

Completing the graph:

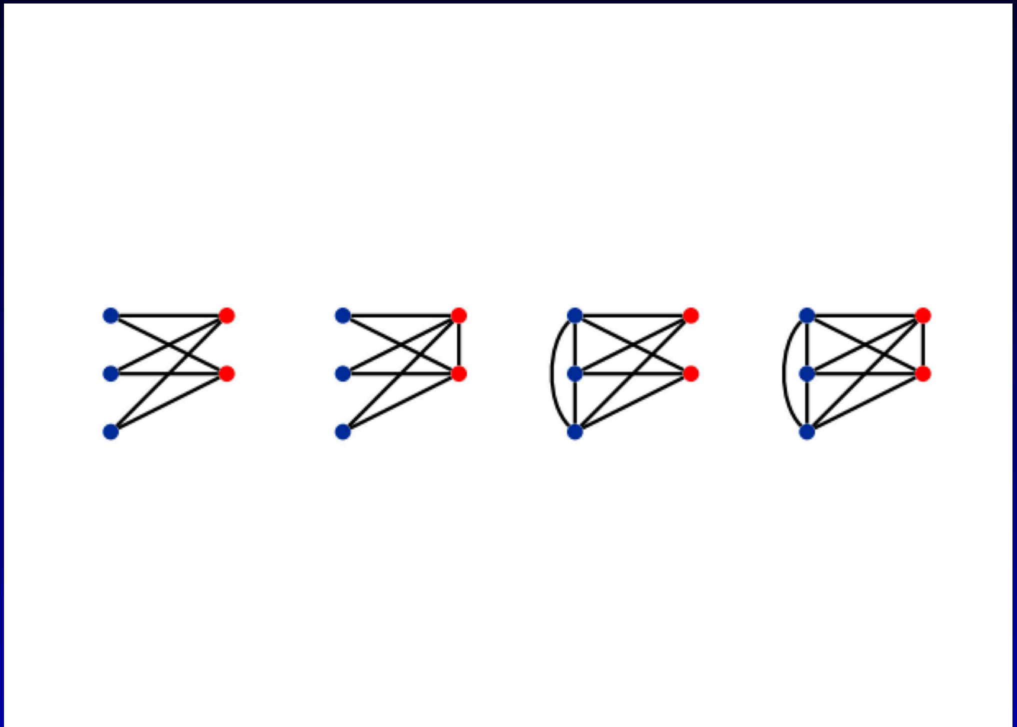

We can extend the models to include tunneling terms while retaining integrability

Integrability: Formal definition

It is generally accepted that an integrable system is one which is derived from a set of commuting transfer matrices.

This definition applies to many-body systems.

Transfer matrix $\tau(u)$: is a generating function of conserved quantities

- The condition:

$$[\tau(u), \tau(v)] = 0$$

- represents a set of conservation laws:

$$[c_n, c_m] = 0$$

- where the series expansion was taken:

$$\tau = \sum_n c_n v^n$$

Quantum Integrable Models:

- Definition:
  A system with L degrees of freedom and Hamiltonian H is quantum integrable if it possesses a set of L independent commuting quantum operators $\{Q_1 = H,\, Q_2,\, \dots Q_L\}$, i. e.

$$[Q_i,\, Q_j] = 0, \;\; \forall \; 1 \leq i, j \leq L$$

- *They can be solved exactly by Bethe Ansatz methods.*

Integrability:

- Classical Mechanics

  If a system with n degrees of freedom possesses n independent first integrals of motion in involution (i.e. Poisson-commuting), then the system is integrable (Liouville)

- Quantum Mechanics: Common definitions

  - 1) A system is quantum integrable if it possesses a maximal set of independent commuting quantum operators $Q_\alpha, \alpha = 1, \dots dim(H)$.
  - 2) A system is quantum integrable if it is exactly solvable, in other words if we can construct its full set of eigenstates explicitly.
  - 3) A system is quantum integrable if it can be mapped to harmonic oscillators.
  - 4) A system is quantum integrable if the scattering it supports is nondiffractive.
  - 5) A system is quantum integrable if its energy level statistics is Poissonian.
  - 6) A system is quantum integrable if it shows level crossings (i.e. does not show level repulsion).

BA-solution: 4 wells

- The model admits multiple pseudovaccum states:

$$|\phi_{k,l}\rangle = (\Gamma^\dagger_{2,4})^k(\Gamma^\dagger_{1,3})^l|0,0,0,0\rangle, \quad k+l \leq N$$

$$\Gamma^\dagger_{1,3} = \alpha_3 a^\dagger_1 - \alpha_1 a^\dagger_3, \quad \Gamma^\dagger_{2,4} = \alpha_4 a^\dagger_2 - \alpha_2 a^\dagger_4,$$

- Other independent conserved operators:

$$Q_{1,3} = \frac{1}{\alpha_1^2+\alpha_3^2}\Gamma^\dagger_{1,3}\Gamma_{1,3}$$

$$Q_{2,4} = \frac{1}{\alpha_2^2+\alpha_4^2}\Gamma^\dagger_{2,4}\Gamma_{2,4}.$$

These operators satisfy the commutation relations

$$[Q_{1,3}, Q_{2,4}] = 0, \quad [H, Q_{1,3}] = [H, Q_{2,4}] = [N, Q_{1,3}] = [N, Q_{2,4}] = 0$$

Appendix: Feasibility of the integrability condition:

- U_0: coupling for on-site interactions which results from contact and DDI interactions Both of these can be either attractive or repulsive, which in principle allows for the manufacture of weak net on-site interaction.
- $U_{ij} = U_{ji}$, $i \neq j$ characterize DDI between particles on different sites.
- Although the DDI follows an inverse cubic law, it is also dependent on the angle between dipole orientation and the displacement between dipoles.
- In combination with the geometry of the trap potential (viz. oblate versus prolate), it is entirely feasible to adjust the system parameters across a wide range of values.
- Importantly, this includes the possibility for the inter-well couplings U_{ij} to have greater magnitude than the on-site coupling U_0.

Appendix: Calculation of the parameters

Consider the Hamiltonian

$$\begin{aligned} H &= \int d^3\vec{r}\,\Psi^\dagger(\vec{r})\left(H_0 + V_{ext}(z)\right)\Psi(\vec{r}) + \frac{1}{2}\int d^3\vec{r} d^3\vec{r'}\Psi^\dagger(\vec{r})\Psi^\dagger(\vec{r'})V(\vec{r}-\vec{r'})\Psi(\vec{r'})\Psi(\vec{r}), \\ &= H_1 + H_2 + H_3, \end{aligned}$$

where

$$\begin{aligned} H_1 &= \int d^3\vec{r}\,\Psi^\dagger(\vec{r})H_0\Psi(\vec{r}), \\ H_2 &= \int d^3\vec{r}\,\Psi^\dagger(\vec{r})V_{ext}(z)\Psi(\vec{r}), \\ H_3 &= \frac{1}{2}\int d^3\vec{r} d^3\vec{r'}\Psi^\dagger(\vec{r})\Psi^\dagger(\vec{r'})V(\vec{r}-\vec{r'})\Psi(\vec{r'})\Psi(\vec{r}), \end{aligned}$$

and

$$H_0 = -\frac{\hbar^2}{2m}\nabla^2 + V_{trap}(r,z).$$

The distance between two nearest wells is d. The interaction potential is given by

$$V(\vec{r}-\vec{r'}) = V_{sr}(\vec{r}-\vec{r'}) + V_{dd}(\vec{r}-\vec{r'}),$$

where the short-range potential is

$$V_{sr}(\vec{r}-\vec{r'}) = g\delta(\vec{r}-\vec{r'}),$$

and the dipole-dipole interaction potential is

$$V_{dd}(\vec{r}-\vec{r'}) = \frac{C_{dd}}{4\pi}\frac{(1-3\cos^2\theta_p)}{|\vec{r}-\vec{r'}|^3}.$$

where $g = 4\pi\hbar^2 a/m$, a is the s-wave scattering length, $C_{dd} = \mu_0\mu^2$, μ is the magnetic dipole moment, μ_0 is the permeability of vacuum and θ_p is the angle between the magnetic dipole moment (which is fixed in z direction) and the vector $(\vec{r}-\vec{r'})$. For ^{52}Cr [3], which has permanent magnetic dipole moment $\mu = 6.0\,\mu_B$, the dipolar length $a_{dd} \equiv (\frac{\mu_0\mu^2}{4\pi})\frac{m}{3\hbar^2} = 16\,a_B$, where $\mu_B = \frac{e\hbar}{2m_e} \approx 9.274\times 10^{-24} J/T$ $(T = 10^4 G)$ is the Bohr magneton and $a_B = \frac{4\pi\epsilon_0\hbar^2}{m_e e^2} \approx 5.292\times 10^{-11} m$ $(m = 10^6 \mu\mathrm{m})$ is the Bohr radius. Consider the ratio $\varepsilon_{dd} \equiv \frac{a_{dd}}{a} = \frac{C_{dd}}{3g} = 0.16$, then $a = 16\,a_B/0.16 = 100\,a_B = 5.292$ nm.

Appendix: Calculation of the parameters

Using the *tight-binding approximation*

$$\Psi(\vec{r}) = \sum_{i=1}^{3} \phi_i(\vec{r}) a_i,$$

where $\phi_i(\vec{r}) = w_0(\vec{r} - \vec{r_i})$ is the localized Wannier function in the center of well i for a single particle. We are assuming the energies involved are not strong enough such that the atom can be kept in the lowest vibrational state (first band). The localized Wannier function is the ground state of H_0 with harmonic approximation.
The first term of H becomes

$$H_1 = \int d^3\vec{r}\, \Psi^\dagger(\vec{r}) H_0 \Psi(\vec{r}) = -\sum_{i,j=1}^{3} J_{ij} a_i^\dagger a_j,$$

where

$$J_{ij} = -\int d^3\vec{r} \phi_i^*(\vec{r}) H_0 \phi_j(\vec{r}).$$

Appendix: Calculation of the parameters

Summing up, the hamiltonian reduces to

$$H = \frac{U_0}{2}\sum_{i=1}^{3} N_i(N_i-1) + \sum_{i=1}^{3}\epsilon_i N_i + U_{12}N_1N_2 + U_{23}N_2N_3 + U_{13}N_1N_3 - (J-\epsilon_{12})(a_1^\dagger a_2 + a_2^\dagger a_1) - (J-\epsilon_{23})(a_2^\dagger a_3 + a_3^\dagger a_2),$$

where

$$\begin{aligned}
J &= -\int d^3\vec{r}\,\phi_1^*(\vec{r})H_0\phi_2(\vec{r}),\\
U_0 &= U_{sr} + U_{dip},\\
U_{sr} &= g\int d^3\vec{r}|\phi_1(\vec{r})|^4, \qquad U_{dip} = \int d^3\vec{r}d^3\vec{r'}|\phi_1(\vec{r})|^2|\phi_1(\vec{r'})|^2 V_{dd}(\vec{r}-\vec{r'}),\\
U_{ij} &= \int d^3\vec{r}d^3\vec{r'}|\phi_i(\vec{r})|^2|\phi_j(\vec{r'})|^2 V_{dd}(\vec{r}-\vec{r'}),\\
\epsilon_{ij} &= \int d^3\vec{r}\,\phi_i^*(\vec{r})V_{ext}(z)\phi_j(\vec{r}), \qquad j = i+1, \qquad i = 1,2\\
\epsilon_i &= \int d^3\vec{r}\,V_{ext}(z)|\phi_i(\vec{r})|^2, \qquad i = 1,2,3.
\end{aligned}$$

By symmetry, $U_{12} = U_{23} = U_1$. At the limit where the distance $d \gg r$, where r is the radius of atomic cloud, we have

$$\begin{aligned}
U_{ij} &= \int d^3\vec{r}d^3\vec{r'}|\phi_i(\vec{r})|^2|\phi_j(\vec{r'})|^2 V_{dd}(\vec{r}-\vec{r'}) \approx (1-3\cos^2\theta_p)\bar{U}_{ij}\\
\bar{U}_{ij} &= \frac{C_{dd}}{4\pi}\int d^3\vec{r}d^3\vec{r'}|\phi_i(\vec{r})|^2|\phi_j(\vec{r'})|^2\frac{1}{|\vec{r}-\vec{r'}|^3}.
\end{aligned}$$

Thus,

$$\frac{U_{12}}{U_{13}} \approx \frac{\int d^3\vec{r}d^3\vec{r'}|\phi_1(\vec{r})|^2|\phi_2(\vec{r'})|^2\frac{1}{d^3}}{\int d^3\vec{r}d^3\vec{r'}|\phi_1(\vec{r})|^2|\phi_3(\vec{r'})|^2\frac{1}{(2d)^3}} = 8 \qquad \Rightarrow \qquad U_{13} = \frac{U_{12}}{8} = \frac{U_1}{8}.$$